PNNL-13483

Pacific Northwest
National Laboratory
Operated by Battelle for the
U.S. Department of Energy

Formulation Efforts for Direct Vitrification of INEEL Blend Calcine Waste Simulate: Fiscal Year 2000

J. V. Crum
J. D. Vienna
Pacific Northwest National Laboratory

D. K. Peeler
I. A. Reamer
Savannah River Technology Center, Aiken, SC 29808

March 2001

Prepared for the U.S. Department of Energy
under Contract DE-AC06-76RL01830

DISCLAIMER

PACIFIC NORTHWEST NATIONAL LABORATORY
operated by
BATTELLE MEMORIAL INSTITUTE
for the
UNITED STATES DEPARTMENT OF ENERGY
under Contract DE-AC06-76RLO 1830

PNNL-13483

Formulation Efforts for Direct Vitrification of INEEL Blend Calcine Waste Simulate: Fiscal Year 2000

J. V. Crum and J. D. Vienna

Pacific Northwest National Laboratory, Richland WA 99352

D. K. Peeler and I. A. Reamer

Savannah River Technology Center, Aiken, SC 29808

March 2001

Prepared for the U.S. Department of Energy
under Contract DE-AC06-76RLO 1830

Pacific Northwest National Laboratory
Richland, Washington 99352

Summary

This report documents the results of glass-formulation efforts for Idaho National Engineering and Environmental Laboratory (INEEL) high level waste (HLW) calcine. Two waste compositions were used during testing. Testing started by using the Run 78 calcine composition and switched to Blend calcine composition when it became available. The goal of the glass-formulation efforts was to develop a frit composition that allows a waste loading exceeding 35 mass% and satisfies the following glass-processing and product-acceptance constraints:

1. Melting temperature of 1125 ± 25°C
2. Viscosity between 2 and 10 Pa·s at the melting temperature
3. Liquidus temperature at least 100°C below the melting temperature
4. Normalized release of B, Li, and Na each below 1 g/m^2 (per ASTM C 1285-97).

Glass-formulation efforts tested several frit compositions with variable waste loadings of Run 78 calcine waste simulant. Frit 107 was selected as the primary candidate for processing since it met all process and performance criteria up to 45 mass% waste loading. When the Blend calcine waste composition became available, Frit 107 and 108 compositions were retested, and again Frit 107 remained the primary candidate. However, both frits suffered a decrease in waste loading (i.e., 40 mass%) when switching from the Run 78 calcine to Blend calcine waste composition. This was due to increased concentrations of both F and Al_2O_3 along with a decrease in CaO and Na_2O in the Blend calcine waste, all of which have strong impacts on the glass properties that limit waste loading of this type of waste.

During testing, waste loading was primarily limited by the propensity to phase separate and/or crystallize fluorine-containing phases at melting temperature or upon cooling. Also of concern was achieving a viscosity between 2 and 10 Pa·s at a melting temperature of 1125 ± 25°C. As waste loading was increased, viscosity was decreased, primarily because of increased concentrations of fluorine (F) for a fixed frit. Also, to retain F, adjustments to frit composition resulted in lowering the viscosity. To meet all processing and product acceptance constraints, melting temperatures of 1050 – 1100°C were utilized.

Table S1 shows the measured properties of glass with Frit 107 at 40 mass% waste loading. Normalized releases of B, Li, and Na for Frit 107 at 40 mass% waste loading are well below the 1 g/m^2 upper constraint for quenched and canister centerline cooling (CCC) heat-treated glass. Also, all of the glass-processing constraints were satisfied with the exception of viscosity. Viscosity is below the 2 Pa·s lower limit at the suggested melting temperature of 1100°C. The preferred melting temperature of the glass is 1050°C, but 1100°C is suggested to maintain $T_M \geq T_L + 100°C$. It is recommended that Frit 107 at 40% waste loading be used for the upcoming melter demonstration.

Table S1. Characterization of Glass with Frit 107 at 40 mass% Waste Loading of Simulated Blend Calcine Waste

Property or Test	**Measured Value**
Quenched glass	100% Amorphous
CCC heat treated glass	~ up to 2 mass% CaF_2
Phase separation temperature	773°C
T_L	~1004°C
Average r_B for quenched glass	0.0315 g/m^2
Average r_{Li} for quenched glass	0.0968 g/m^2
Average r_{Na} for quenched glass	0.1134 g/m^2
Average r_B for CCC glass	0.0532 g/m^2
Average r_{Li} for CCC glass	0.1279 g/m^2
Average r_{Na} for CCC glass	0.0967 g/m^2
Viscosity at 1100°C	1.47 Pa·s
Electrical conductivity at 1100°C	31.53 S/m
Glass transition temperature	419°C
Softening point	492°C
Density	2.72 g/cm^3
Devitrification at 750°C/48 h	Estimated to be 90 vol% crystallized
Remelt of devitrification sample at 1000°C/1 h	100% amorphous

Glossary

η	viscosity
ASTM	American Society for Testing and Materials
BDAT	best demonstrated available technology
CCC	canister centerline cooling
CSSF	calcined solids storage facilities
DOE	U.S. Department of Energy
DTA	differential thermal analysis
DWPF	Defense Waste Processing Facility
EA	environmental assessment
EDS	energy dispersive spectroscopy
EIS	environmental impact statement
EPA	U.S. Environmental Protection Agency
GC	gas chromatograph
HAW	high-activity waste
HLW	high-level waste
IC	ion chromatography
ICPP	Idaho Chemical Processing Plant
INEEL	Idaho National Engineering and Environmental Laboratory
INTEC	Idaho Nuclear Technology and Engineering Center
LOI	loss on ignition
ML	maximum waste loading
MS	mass spectrometer
NL	normalized loss
OM	optical microscopy
PCT	product consistency test
PNNL	Pacific Northwest National Laboratory
r_B	normalized release rate of boron

RCRA	Resource Conservation and Recovery Act
ri	normalized release
r_{Li}	normalized release rate of lithium
r_{Na}	normalized release rate of sodium
SEM	scanning electron microscope
SRTC	Savannah River Technology Center
T_g	glass transition temperature
T_L	liquidus temperature
T_M	nominal melter operating temperature
T_s	softening point temperature
TGA	thermogravimeteric analysis
WAPS	Waste Acceptance Product Specification
WC	tungsten carbide
WL	waste loading
WVDP	West Valley Demonstration Project
XRD	X-Ray diffraction

Acknowledgments

The authors would like to acknowledge the following people:

- Lynette Jagoda, Mike Schweiger, and Don Smith for laboratory assistance
- Wayne Cosby for editorial assistance
- Dong-Sang Kim and Brad Scholes technical review
- E. William Holtzscheiter for management and guidance

This study was funded by the Department of Energy's (DOE's) Office of Science and Technology, through the Tanks Focus Area, and office of Waste management through the Idaho National Environmental and Engineering Laboratory high-level waste program. This study was performed and documented as a collaborative effort by Pacific Northwest National Laboratory (operated for DOE by Battelle under Contract DE-AC06-76RLO 1830), Westinghouse Savannah River Company (operated for DOE under Contract (DE-AC09-96SR18500) and Idaho National Environmental and Engineering Laboratory (operated for DOE by Bechtel, Babcox and Wilcox Incorporated under contract DE-AC07-94ID 13223).

Contents

Figures

Tables

1.0 Introduction

The Idaho National Engineering and Environmental Laboratory (INEEL) High-Level Waste Technology Development program has the goal of defining processes that are capable of immobilizing Idaho Nuclear Technology and Engineering Center (INTEC) high-level wastes (HLWs) to a qualified waste form that will be road ready for disposal before Year 2035. INTEC, formerly known as the Idaho Chemical Processing Plant (ICPP), reprocessed spent nuclear fuel to recover fissionable uranium. Liquid-waste raffinates from reprocessing were converted to a granular solid (calcine). This calcine is considered a mixed hazardous waste under current Resource Conservation and Recovery Act (RCRA) regulations. Approximately 4,400 m^3 of calcine are presently being stored in stainless steel bins at INTEC. The calcine solids were sent to storage in stainless steel bins located in concrete vaults to isolate them from the environment. The bins are designed to remove the heat generated by the radioactive decay of fission products (1% by weight) in the calcine. Several calcined solids storage facilities (CSSF) have been constructed over the years. To date, six CSSFs are being used to store the calcine. Each CSSF design is different in that each CSSF includes a range of three to seven composite bin and sub-bins. In addition to the design differences, each bin includes the following internal obstructions that may hinder the retrieval process: multiple thermowells, wall stiffeners, braces, and corrosion coupons. The calcine compositions in these CSSFs vary, depending on feed composition to the calcine. Therefore, the calcine types are layered in the binsets; thus, the compositions defined by CSSF are reported as composite composition. For the studies documented in this report, a Blend calcine composition was used resulting from a specific retrieval strategy/blending scenario.[(a)]

The U.S. Environmental Protection Agency (EPA) has identified vitrification, the process of converting waste into a glass, as the best demonstrated available technology (BDAT) for immobilizing wastes generated during the reprocessing of nuclear fuel. The Batt Settlement Agreement between the State of Idaho, the U.S. Department of Energy (DOE), and the Navy states that all HLW calcine must be treated and considered road ready for repository storage by 2035. New technologies are necessary to successfully design a waste-treatment facility that will meet these INEEL regulatory milestones. Two requirements are to develop (1) glass formulations and (2) integrated vitrification flowsheets that will successfully immobilize INEEL HLWs. The definitions of these glass formulations and integrated flowsheets have been initiated by a cooperative testing program between INEEL, Savannah River Technology Center (SRTC), and Pacific Northwest National Laboratory (PNNL). One of the

(a) Although a simulated Blend calcine composition was the focus of this study, the composition was not finalized until after the study was initiated. Run 78 calcine was used for the first portion of the study because of the expected similarities in composition.

environmental impact statement (EIS) options being considered as the treatment process for immobilizing INEEL HLW is early vitrification, which includes direct vitrification (bypass pretreatment of waste) of INEEL calcine. This report documents the Fiscal Year 2000 (FY00) activities for developing glass forms to demonstrate the direct vitrification of INEEL Blend pilot plant calcine.

2.0 Waste Composition

Based on the information from the calcine blending assessment (Staiger 1999) and existing calcine analytical data, INEEL provided the Blend calcine composition to be used for the glass-formulation efforts (see Table 2.1). The Blend calcine composition is based on a retrieval and blending (fully homogenized) scenario that is theoretically possible. The retrieval/blending strategy was performed by Nelson, Mohr, and Taylor (Mohr et al. 2000) using a Monte Carlo simulation in which the primary objective was to minimize the standard deviation for three key calcine components: Al, Zr, and F. Although the goal of the blending assessment was to minimize variation in Al, Zr, and F via retrieval from a given number of binsets, realistically, variation in both the major and minor components will be significant. However, the nominal-Blend calcine composition (shown in Table 2.1) is expected to fall within the range of "actual" calcine batches, given that direct vitrification is pursued. For the purposes of this study, we've normalized components expected to remain in glass to oxides, F and Cl.

The Blend calcine is dominated by five major components: Al_2O_3, CaO, F, ZrO_2, and SO_3. Also shown in Table 2.1 are the average values for the major components associated with the Run 78 calcine waste. Comparing the two waste compositions, concentrations of Al_2O_3 and F are higher and CaO is lower in the Blend calcine while ZrO_2 and SO_3 remained essentially the same. Previous glass-formulation efforts developed a 38 mass% loaded glass for the Run 78 calcine waste stream (Musick et al. 2000). Musick et al. used a self-imposed limit of ≤ 2 vol% of crystals after a simulated canister centerline cooling (CCC) heat treatment: although there was no negative impact on durability as defined by the product consistency test (PCT) at higher vol% crystallinity. This crystallinity constraint ultimately limited waste loading of Run 78 calcine to 38 mass%.

Table 2.1. Composition of Blend Calcine and Run 78 Calcine

	Blend Calcine	**Run 78 Calcine**
Oxide	**Mass %**	**Mass %**
Al_2O_3	32.06	24.71
B_2O_3	2.30	1.92
CaO	27.95	33.44
CoO	0.04	-
Cs_2O	0.26	-
F	14.90	13.46
Fe_2O_3	0.57	0.77
K_2O	0.54	0.41
MgO	0.83	-
MnO	0.03	0.36
Na_2O	3.05	4.38
NiO	0.73	0.09
P_2O_5	0.43	3.36
SnO_2	0.20	-
SrO	0.24	-
ZrO_2	13.54	13.53
SO_3	2.22	2.26
Cl	0.11	0.11
Total	*100.00*	*98.80*

3.0 Glass-Property Restrictions

With the goal of developing an acceptable glass waste form to demonstrate the direct vitrification of INEEL Blend calcine, we must first establish a definition of an acceptable glass. Two types of glass-property limitations must be considered: 1) those product properties required for waste-form acceptance and 2) those processing properties required to ensure adequate melter processability. The product properties are dictated by the Waste Acceptance Product Specification (WAPS) (DOE 1995). The WAPS imposes limitations on the performance of glass in the PCT (ASTM 1998) and requires that chemical and phase-stability information be reported. The specific limit is that the releases of boron, sodium, and lithium, normalized to glass composition, (r_B, r_{Na}, r_{Li}) must be at least "2 standard deviations" less than those of the Defense Waste Processing Facility (DWPF) environmental assessment (EA) glass (Jantzen et al. 1993). This implies that these releases must be controlled to at least the 95% confidence level after accounting for appropriate uncertainties. Values of r_B, r_{Na}, and r_{Li} for the DWPF-EA glass are 8.35 (g/m^2), 6.67 (g/m^2), and 4.78 (g/m^2), respectively (Jantzen et al. 1993). Without information specific to the operation of a glass plant at INEEL, it is difficult to assess all of the uncertainties that must be accounted for in the release values. For the purposes of this study, we will take 1 g/m^2 as a conservative limit for r_B, r_{Na}, and r_{Li}.

A specific limit on crystallinity in the glass product has not been specified by the WAPS. However, the formation of crystals in glass during canister cooling may affect chemical durability. The primary concerns with the formation of crystals upon canister cooling are the ability to specify the phases present in the waste form and their compositions and to predict the durability of the final waste form. For these reasons, we have imposed the conservative 1 g/m^2 limit for r_B, r_{Na}, and r_{Li} for the acceptable release limits after CCC. As previously noted, earlier studies (Musick et al. 2000) used a $\leq$ 2 vol% upper limit on crystallinity after CCC as a temporary guide for initial glass-formulation efforts. This limit was found to be overly restrictive in terms of waste loading because of the minimal impact of crystalline-phase formation on durability (for the glass compositions tested) as determined by follow-on work. The time-temperature schedule assumed for CCC in these glass-formulation efforts is given in Table 3.1. The current study will not impose the 2 vol% crystallization limit after CCC, but will use the conservative 1 g/m^2 limit for r_B, r_{Na}, and r_{Li} as the acceptable release limits for both quenched and CCC heat-treated glasses. In addition, the crystallinity of glasses subject to the CCC schedule will be reported.

It is difficult to set limits on processing properties without knowing the specific processing technology to be used for high-activity waste (HAW) vitrification at INEEL. We will let the HAW vitrification experience at the DWPF and West Valley Demonstration Project (WVDP) as well as recent glass-formulation studies with INEEL high F-based wastes (Musick et al. 2000) be our guide and/or basis. For the operating HAW vitrification plants at DWPF and WVDP, the nominal melter operating temperature (T_M) is maintained at or close to 1150°C. However, glass-formulation efforts for Run 78

calcine indicated that melt viscosity decreased, resulting in a decreased T_M, as waste loadings increased (Musick et al. 2000). This was primarily a result of the high F concentration in the Run 78 calcine waste (see Table 2.1). In that study, we did not limit the operating temperature since existing technologies have demonstrated the capability of vitrifying waste at higher and lower temperatures. However, we determined an acceptable glass composition for processing Run 78 calcine at a reasonable loading (e.g., 38 mass% on a non-volatile, oxide basis) and then determined the optimum fabrication temperature (i.e., 1050°C) based on the viscosity-temperature relationship.

With an estimated F concentration of 14.9 mass% in the Blend calcine composition (see Table 2.1), the goal of increasing waste loading (relative to 38 mass% for Run 78 calcine) will most likely result in a decrease in T_M. Previous studies have demonstrated that F solubility increases by increasing alkali (Na_2O and/or Li_2O) and/or CaO concentrations to a base glass while increasing SiO_2, Al_2O_3 and/or ZrO_2 concentration decreases F solubility (Musick et al. 2000) as shown in Figure 3-1. These data suggest that to increase F solubility, components that ultimately reduce T_M should be added. With this dilemma in mind, glass-formulation efforts attempted to meet the primary goals of increasing melting temperature to 1125 ± 25°C while maintaining relatively high waste loadings.

Table 3.1. Time/Temperature Schedule of Simulated CCC

Segment	Ramp (°C/h)	Level (°C)	Dwell (h)
1	-	1150	0.33
2	0.2	925	0.1
3	2.5	779	2.8
4	1	715	3.4
5	2	598	4.2
6	1.8	490	4.3
7	1.8	382	7.4

The viscosity (η) at T_M is maintained between 2 and 10 Pa·s in both the DWPF and WVDP glasses and will be maintained in this range for the INEEL Blend calcine glass. Maintaining the viscosity within these limits is important as it has major influence on the melting rate of melter feeds, and corrosion of refractories and electrodes. Melt viscosity also dectates the rates of bubble release (foaming and fining) and homogenization. If the viscosity is too low, excessive convection currents can occur, increasing corrosion/erosion of the melter materials (electrodes and refractories) and making control of the melter more difficult. Finally, the liquidus temperature (T_L) of glass in the melter is maintained at a minimum of 100°C below the nominal operating temperature.

The restrictions on ri [both quenched and CCC], η, T_M, and T_L are the primary constraints adopted for this study in developing an acceptable glass. An additional processing-related concern is the corrosion of melter material during processing. Before pilot-scale melter demonstrations, these concerns should be addressed to ensure that excessive corrosion will not be encountered. Characterizing the corrosion of melter-construction materials is beyond the scope of this study. Long-term material corrosion tests will

be necessary before final adaptation of the vitrification technology once the final waste-treatment flowsheets have been developed.

Once a specific glass composition meets all of the primary constraints listed above, other tests may be used to further reduce the technical risk of melter processing. Tests can be performed to evaluate the effects of compositional uncertainties on these primary processing and product-performance properties. The uncertainties (both measurement and sampling) associated with the HAW compositional analysis, potential feed variability, the effect of volatilization of critical components, and potential batching errors (i.e., waste-loading variations) can be addressed to some degree via laboratory tests. These tests can reduce the technical risks of processing a specific glass composition through a given melter, but it should be recognized that these risks are not eliminated. This is because of the differences between laboratory-scale testing and actual melter processing.

Table 3.2 summarizes the glass-property and composition constraints used to develop a glass for demonstrating direct vitrification of Blend calcine.

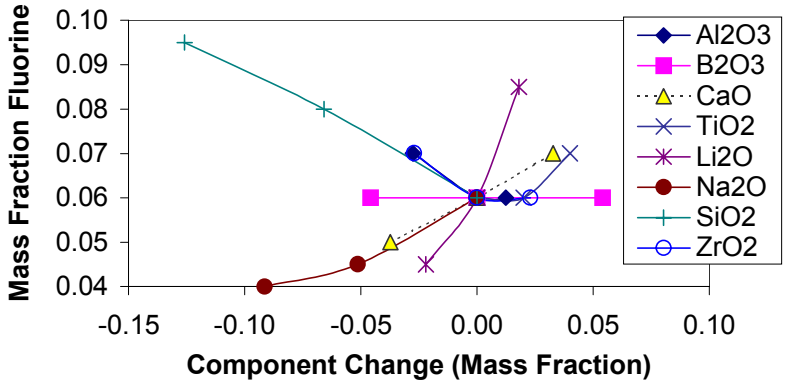

Figure 3-1. Effect of Component Concentration Change to Base Glass on F Solubility

Table 3.2. Constraints Used in Blend Calcine Glass Formulation

Property	Property limit
η at T_M	$2<\eta<10$ Pa·s
T_L	$T_M - 100^{\circ}C$
PCT r_B	$r_B < 1$ g/m^2
PCT r_{Na}	$r_{Na} < 1$ g/m^2
PCT r_{Li}	$r_{Li} < 1$ g/m^2

4.0 Glass-Formulation Scoping Studies with Run 78 Calcine

Preliminary glass-formulation studies were performed using the Run 78 calcine composition shown in Table 2.1. These scoping studies assumed that the Run 78 calcine composition would be similar to that of the Blend calcine in terms of F and/or CaO concentration.[(a)]

The initial goals of these studies were twofold:

- increase the waste loading relative to the Run 78 calcine glass composition (38 mass%)
- increase the melting temperature (1125 ± 25°C).

As previously noted, these two goals may counter each other because of the composition of the waste stream being treated (e.g., high F-based waste results in lower melt temperatures as waste loadings increase).

The glass-formulation activities associated with the Run 78 calcine waste were an obvious starting point for the Blend calcine. Three frits (Frit 5, 9 and 10) were developed and successfully processed in a pilot-scale melter at Clemson University with the Run 78 calcine waste (Musick et al. 2000). The compositions of Frits 5, 9, and 10 as well as the five new scoping-study frits (for this study) are shown in Table 4.1.

The composition variation of the maximum waste loading (ML) frits was initially focused on evaluating the potential to increase the melting temperature while maintaining F solubility limits. This was accomplished by reducing the amount of total alkali (and their relative proportions) as well as varying the SiO_2 concentration. Given the minimal impact of the B_2O_3 and Fe_2O_3 concentration on F solubility (see Figure 3-1), their concentration in the five ML frits was varied to account for alkali and SiO_2 variations.

Initial loadings of 50 mass% using the Run 78 calcine composition[(a)] were targeted. Although devitrification upon CCC was anticipated, previous results (Musick et al. 2000) indicated that up to 20–30

(a) This assumption would later be proven invalid as both the F and CaO concentrations for the Blend calcine would exceed that of the Zr-calcine. Given the higher concentrations of F and CaO, the goal of increasing waste loading relative to the 38 mass% is perhaps an unfair comparison, given that F should dictate waste loading.

Table 4.1. Initial Frit Compositions

Frit	SiO_2	Na_2O	Li_2O	B_2O_3	Fe_2O_3	La_2O_3	ZrO_2
5	64.61	15.16	9.23	6.80	4.20	0.0	0.0
9	59.3	14.6	10.0	10.5	0.0	4.0	1.6
10	59.3	14.6	10.0	10.5	4.0	0.0	1.6
ML-102	80.0	5.0	5.0	10.0	0.0	0.0	0.0
ML-103	70.0	4.0	10.0	10.0	4.0	0.0	2.0
ML-104	65.0	4.0	10.0	15.0	4.0	0.0	2.0
ML-105	60.0	8.0	10.0	15.0	5.0	0.0	2.0
ML-106	70.0	12.0	6.0	10.0	0.0	0.0	2.0

vol% crystallization had no negative impact on durability. In fact, durability increased for Frit 9 and 10 as waste loading and the resulting crystallinity increased. Within the composition region tested, durability generally improves with increased crystallization. However, the effect of crystallization on durablity varies, dependent on crystal type and concentration and the effect on the remaining glass composition. The remaining glass composition generally determines the durablity of the crystallized glass (Baliey and Hrma 1995, Hrma and Bailey 1995 , Kim et al. 1995, and Li et al. 1997).

Glasses were fabricated using oxides, carbonates, and boric acid precursors according to standard procedures. The glasses were melted for 1 h at 1150°C in a covered Pt/Rh crucible, quenched on a steel plate, ground in a tungsten carbide (WC) mill, remelted for 1 h, and quenched on a steel plate. The resulting pour patty was then used as stock for obtaining samples for the various property measurements.[(b)] Although viscosity was not measured, all glasses (with the exception of ML-106) poured well at 1150°C.[(c)]

(a) The specific Zr-calcine composition used is listed as Composition "D" in Table 2.3 of INEEL/EXT-2000-00110.
(b) Observations of the resulting pour patty and crucible remains can be found in the laboratory notebook (WSRC-NB-99-00235).
(c) ML-106 poured well when processed at 1200°C.

Table 4.2. summarizes the homogeneity (visual and x-ray diffraction [XRD]) of the as-fabricated (quenched) ML glasses. All five glasses were visually characterized as opaque, resulting from either undissolved solids or amorphous and/or crystalline phase separation. Visual observations for homogeneity were documented, and representative samples from each as-fabricated glass were analyzed by XRD to determine crystal types.[a] Baddeleyite (ZrO_2) and fluoride-based phases (e.g., CaF_2 and $Ca_{10}(SiO_4)_3(SO_4)_3F_2$) were detected by XRD. After evaluating the glasses via optical microscopy (OM), it was determined that the ZrO_2 appeared to be present as undissolved solids while the F-based crystals had a well-defined morphology indicating thay were crystallized during melting or cooling.

Table 4.2. Visual and XRD Results of Initial Scoping Study Glasses

Glass	Visual	XRD
ML-102-50 (1)	Opaque	CaF_2, $ZrSiO_4$, $Ca_5(PO_4)_3F$
ML-103-50	Opaque	CaF_2, ZrO_2 (2)
ML-104-50	Opaque	CaF_2, ZrO_2
ML-105-50	Opaque	CaF_2, ZrO_2
ML-106-50	Opaque	CaF_2, ZrO_2

(1) "-50" indicates glasses targeting 50 mass% loading.
(2) ML-102-50 was the only ML frit that did not contain ZrO_2; ZrO_2 not detected in ML-102-50.

Thirty grams of each glass were placed in a platinum/rhodium crucible, heated to 1150°C, held at temperature for 1 h, and then, while in the furnace, allowed to cool to room temperature based on the calculated/measured CCC profile of a DWPF-type canister (Table 3.1) (Marra and Jantzen 1993). The crystallinity and PCT releases of glasses were measured for comparison to their quenched counterpart glasses. The glass-formulation criterion established that the volume-percent of crystalline phases would not be a limiting factor if the durability of the partially crystallized waste form was still adequate (upper limit is ri $\leq$ 1 g/m^2). As expected, the impact of slow cooling allowed significant crystal formation with all CCC glasses being highly devitrified (estimated to be > 80 vol%).

To assess the durability of all quenched and CCC ML glasses, the PCT (ASTM C 1285-97) (ASTM 1998) was performed. The PCT was completed in triplicate for each quenched and CCC glass. Two standard glasses and a blank were included for control purposes. The EA (Jantzen et al. 1993) and Approved Reference Material (ARM-1) (Mellinger and Daniel 1984) were used as the control glasses. Samples were ground, washed, and prepared according to procedure. Fifteen grams of ASTM Type I water were added to 1.5 g of glass in stainless steel vessels. The vessels were tightly sealed, weighed, and placed in an oven at 90°C for 7 days. After the 7 days, vessels were allowed to cool to room temperature, and the final weight of each vessel and the solution pH were recorded. The leachate was filtered through

(a) The run conditions of the XRD instrument were 5° to 70° 2θ with a 0.02 step and a hold of 1 sec per step.

a 45-μm pore size filter and then acidified with 0.4 M HNO_3. Six milliliters of each leachate solution were acidified with 4 mL of 0.4 M HNO_3 to ensure that the cations remained in solution. The solutions were then analyzed for concentrations of B, Li, and Na by ICP-AES.

Normalized releases of B, Li, and Na were then calculated based on target compositions and compared to those limits defined by the EA glass (Jantzen et al. 1993). Table 4.3 summarizes the r_i limits for the EA glass and the self-imposed limits used in this study.

Table 4.3. Reported Normalized Elemental Releases for EA and Constraint Used for this Study

Element	EA (g/m^2)	Study Constraint (g/m^2)
B	8.35	1
Li	4.78	1
Na	6.67	1

Average r_i for the five ML glasses (both quenched and CCC versions) are reported in Table 4.4. All r_i are well below those reported for the EA glass (see Table 4.3) as well as the conservative constraint of 1 g/m^2 being used in this study.

Figure 4-1 shows a plot of r_B (in g/m^2) for the quenched versus CCC ML glasses[(a)]. Based on statistical analysis, there is a statistically significant difference (at the 0.05% level) between the quenched and CCC r_B values. The CCC glasses had on average a 0.25 g/m^2 larger release than (lower durability as defined by PCT) their quenched counterparts.

Table 4.4. PCT Results of ML-102 Through 106 Quenched and CCC Glasses at 50 mass% Loading

Glass ID	r_B (g/m^2)	r_{Li} (g/m^2)	r_{Na} (g/m^2)	pH
ML-102 Q	0.0652	0.4281	-	9.69
ML-102 CCC	0.2670	0.1693	0.0438	9.83
ML-103 Q	0.0787	0.1492	0.0841	10.27
ML-103 CCC	0.4953	0.3643	0.1663	10.31
ML-104 Q	0.0881	0.1544	0.0934	10.18
ML-104 CCC	0.1080	0.1737	0.0902	10.30
ML-105 Q	0.1139	0.1882	0.1485	10.43
ML-105 CCC	0.5997	0.4728	0.2789	10.37
ML-106 Q	0.1067	0.1956	0.1392	10.39
ML-106 CCC	0.2639	0.4545	0.1484	10.08

Based on the needs to minimize crystal fraction (both quenched and CCC), the initial ML scoping study glasses were ranked as follows (best to worst): ML-105, ML-103, ML-104, ML-106, and ML-102. The SiO_2 content for ML-105 was the lowest of all glasses evaluated. The total alkali content was also the highest of the five ML glasses. These compositional variations are consistent

(a) Note that releases in this report have been normalized to both glass composition and glass surface area to solution volume, yielding r_i values in g/m^2. It is also common to normalize concentrations only to glass composition, yielding normalized loss (NL) values in g/L. There is no correct method for normalization, however, since PCT is performed with a fixed ration of glass to water mass; waste forms with different densities are more readily compared if normalized to surface area to volume ratio. To convert from r_i to NL, one can multiply by 2, assuming 2000 m^{-1} of glass surface area in the test ($2 \cdot r_i = NL_i$).

with the results of the F-solubility study in terms of maximizing F solubility (Musick et al. 2000) and avoiding the formation of crystallization (e.g., F solubility increases with decreasing SiO_2 concentration and increasing alkali concentration—see Figure 3-1). These results indicate that increasing melting temperature relative to Frits 5, 9, and 10 studied by Musick et al. (2000) is not favorable to maintaing or improving F solublity in glass.

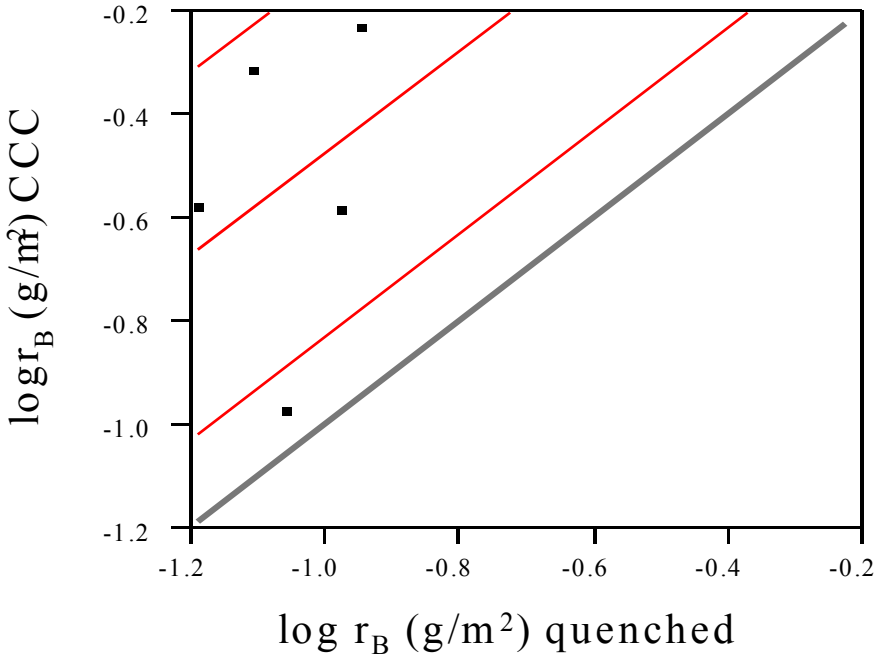

Figure 4-1. Log r_B (in g/m^2) for Quenched Versus CCC ML Glasses

4.1 FRITS 107 and 108 (with Run 78 calcine)

Two additional frits were formulated (ML-107 and ML-108—see Table 4.5) based on the results of the initial scoping tests discussed in the previous section and via model predictions using a limited database within the compositional envelope of interest. Of particular interest is the inclusion of La_2O_3 and TiO_2 to Frits 107 and 108, respectively. The use of La_2O_3 is based on results of developing Frit 9 for Run 78 calcine, which was effective in reducing the devitrification potential upon thermal heat treatment. The use of TiO_2 is expected to help to increase F solubility, glass durability, and η. Additions of either TiO_2 or La_2O_3 are expected to decrease η at high temperatures and increase η at low temperatures.

ML-107 and ML-108 frits have approximately the same total alkali content as ML-105. However, the total alkali content is less than that used in Frits 5, 9, and 10. This again is due to the compositional balance between increasing melt temperature and waste loading while maintaining relatively high F solubility (e.g., waste loading) as well as restricting the total alkali content of the final glass to maintain adequate durability.

Table 4.5. Compositions of Past Successful Frits and Present Formulation Efforts, Given in Mass Fraction Oxides

Frit	SiO_2	Na_2O	Li_2O	B_2O_3	Fe_2O_3	La_2O_3	ZrO_2	TiO_2
5	64.61	15.16	9.23	6.80	4.20	0.00	0.00	0.00
9	59.30	14.60	10.00	10.50	0.00	4.00	1.60	0.00
10	59.30	14.60	10.00	10.50	4.00	0.00	1.60	0.00
ML-105	60.00	8.00	10.00	15.00	5.00	0.00	2.00	0.00
ML-107	61.18	5.62	12.00	14.08	0.62	6.50	0.00	0.00
ML-108	61.18	5.62	12.00	14.08	0.62	0.00	0.00	6.50

Based on the results of Frits ML 102–106, loadings of 45 and 50 mass% were targeted for ML-107 and ML-108. These glasses were fabricated using the same standard procedures described in Section 4.0. All of the glasses poured well at 1150°C.

Table 4.6. summarizes the visual observations of the as-fabricated (quenched) ML-107 and ML-108 glasses as a function of loading. Both glasses targeting 45 mass% loadings appeared to be homogeneous. Glasses targeting 50 mass% loadings were opaque. ML-108-50 glass also contained a small quantity of undissolved solids in the residual crucible glass.

Table 4.6. Visual Results of "As-Fabricated" ML-107 and ML-108 Glasses

Glass	Visual
ML-107-45	Homogeneous
ML-107-50	Opaque
ML-108-45	Homogeneous
ML-108-50	Opaque, undissolved solids

Thirty grams of each glass were placed in a platinum/rhodium crucible and heat treated according to the CCC profile. Visual observations of each glass indicated that ML-107 at 45 mass% loading had the least devitrification (although estimated to be 70-80 vol%). Table 4.7 provides an estimated crystalline vol % and visual description of each glass after CCC. XRD was not performed on this series of glasses.

Table 4.7. Visual Observations of CCC Heat-Treated ML-107 and –108 Glasses

Glass	Estimated Vol% Crystallization	Comments
ML-107-45	70 – 80	Continuous glass phase appears to be present
ML-107-50	> 90	Completely devitrified, no continuous glass phase observed
ML-108-45	> 90	Completely devitrified, no continuous glass phase observed
ML-108-50	> 90	Completely devitrified, no continuous glass phase observed

PCT was performed in triplicate on all quenched and CCC ML-107 and ML-108 glasses. Two standard glasses and a blank were included for control purposes. The r_B, r_{Li}, and r_{Na} values were then calculated based on target compositions and compared to those limits defined by the EA glass (Jantzen et al. 1993) and the self-imposed 1 g/m^2 for both quenched and CCC glasses.

The average r_i values for the two glasses (both quenched and CCC versions) are reported in Table 4.8 as a function of waste loading. All r_i are well below those reported for the EA glass (see Table 4.3). All but one glass (ML-108-50 CCC) meets the conservative 1 g/m^2 constraint after CCC – r_{Li} = 1.2866 g/m^2.

Table 4.8. PCT Results of ML-107 and 108, Quenched and CCC Glasses, at 45 and 50 mass% Loadings

Glass ID	r_B (g/m^2)	r_{Li} (g/m^2)	r_{Na} (g/m^2)	pH
ML-107-45 Q	0.0712	0.1372	0.1901	10.49
ML-107-45 CCC	0.0422	0.1209	0.1701	10.47
ML-107-50 Q	0.0619	0.1185	0.1708	10.44
ML-107-50 CCC	0.1360	0.2047	0.2052	10.53
ML-108-45 Q	0.0653	-	0.0287	10.39
ML-108-45 CCC	0.0744	-	0.0324	10.10
ML-108-50 Q	0.0575	0.1792	0.0626	10.40
ML-108-50 CCC	0.5335	1.2866	0.1866	10.24

Figure 4-2 shows a plot of log [r_B] (in g/m^2) for the quenched versus CCC ML-107 and ML-108 (at 45 and 50 mass% loading) glasses. Based on statistical analysis, there is no indication of a statistically significant difference (at the 0.05% level) between the quenched and CCC r_B release values. The CCC glasses had on average a 0.13 g/m^2 larger release (lower durability as defined by PCT) than their quenched counterparts.

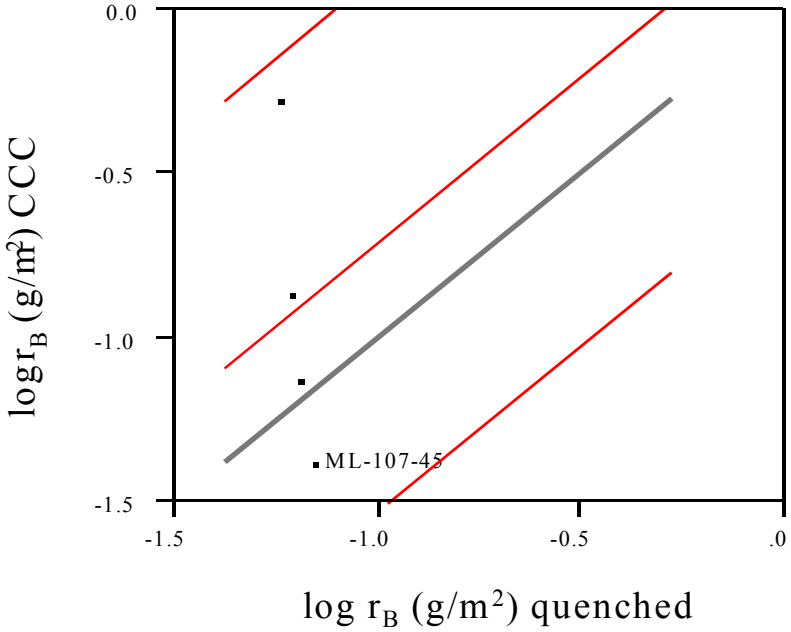

Figure 4-2. Log r_B (in g/m^2) for Quenched Versus CCC ML-107 and ML-108 Glasses

4.2 BLEND CALCINE COMPOSITION

The preliminary glass-formulation effort (Frits ML-102 – ML-108) used Run 78 calcine composition. The Bend calcine composition was used for further studies once it was received. A comparison of the major component concentrations in the two wastes shown in Table 2.1 indicates that CaO and Na_2O concentrations are lower in the Blend calcine while F and Al_2O_3 levels are higher. ZrO_2 and SO_3 concentrations essentially remained constant. As discussed in this section, additional studies were performed to determine the impact of these compositional changes on preliminary glass formulations.

Glasses targeting a loading range of 40–50 mass% using ML-107 and ML-108 and the Blend calcine composition (shown in Table 2.1)[(a)] were fabricated according to standard procedures. All of the glasses poured well at 1150°C.

Table 4.9 summarizes the visual observations of the as-fabricated (quenched) ML-107A and ML-108A glasses as a function of waste loading. The impact of the higher F content (relative to the Run 78 calcine composition) is apparent by the necessary reduction in waste loading (relative to Run 78 calcine results shown in Table 4.6) to produce a visually homogeneous glass. To produce a homogeneous glass, waste loadings in glasses with both Frit ML-107 and Frit ML-108 were reduced to 40 mass% with the Blend calcine down from 45% with the Run 78 calcine composition. As waste loadings increase, glasses change from homogeneous (at 40 mass%), to opaque (at 45 mass%—most likely resulting from devitrification of CaF_2 or other F-based compounds), and finally to opaque with possible undissolved solids (at 50 mass%). This was expected and is consistent with the current knowledge of the effect of F on various properties of waste glasses previously tested.

Given an apparent "homogeneity boundary" between 40 and 45 mass% loading with the Blend calcine, two additional melts were prepared targeting 42 and 44 mass% loading with Frit ML-107. These glasses were fabricated using standard batching and melting procedures previously discussed. Visual observations of homogeneity are summarized in Table 4.9. ML-107A-42 was visually homogeneous. ML-107A-44 is characterized by a thin, homogeneous glass layer on the bottom of the pour patty (interface where the glass was quenched on the stainless steel plate) while the bulk of the glass was opaque. Figure 4-3 shows a cross section of a glass with similar physical characteristics.

(a) To differentiate the glasses fabricated with the Blend calcine composition from those fabricated using the Run 78 calcine composition, an "A" will be placed after frit nomenclature for the glasses made with Blend Calcine.

Table 4.9. Visual Results of "As-Fabricated" ML-107A at 42 and 44 mass% Loading

Glass	Visual
ML-107A-42	Homogeneous
ML-107A-44	Homogeneous at interface, opaque in bulk

The formation of opalescence (most likely due to the formation of CaF_2 or other F-based compounds as shown in Figure 4-3 is highly dependent upon F solubility in glass and thermal history. To ensure that ML-107A-40 and ML-107A-42 were not homogeneous as a result of F volatility during melting, samples of ML-107A-40, -42, and -44 were submitted to the SRTC-ML for full elemental analysis (including F analysis by ion chromatography [IC]). As shown in Table 4.10, measured F concentrations are slightly lower than target values by ~ 9–10 %, which is within the analytical error of the IC. It was concluded that minimal F volatility occurred during fabrication, and homogeneity resulted from complete solubility.

To assess the durability of the ML-107A-42 and -44 glasses, PCT (ASTM 1997) was performed in triplicate for each quenched glass.[(a)] Standard glasses and a blank were included for control purposes. Samples were ground, washed, and prepared according to procedure. Normalized releases of B, Li, and Na were then calculated based on target compositions and compared to those limits defined by the EA glass (Jantzen et al. 1993) and the self-imposed 1 g/m^2.

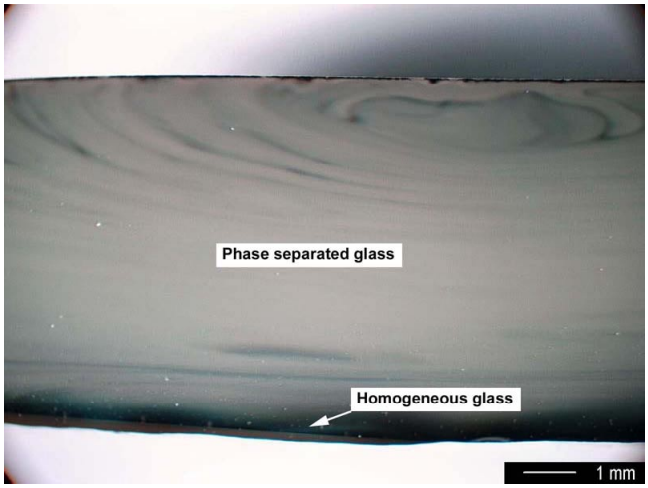

Figure 4-3. Cross Section of High F-Based INEEL Glass. Bulk glass is opaque while a homogeneous glass results at the initial quenched interface

(a) PCTs were only performed on the quenched versions of ML-107A-40, -42, and -44. The effect of CCC on durability was assessed on the candidate frit composition, which is discussed in a later section.

Average normalized elemental releases for ML-107A-40, -42, and -44 glasses are reported in Table 4.11. All normalized releases are well below those reported for the EA glass (see Table 4.3) and the conservative 1 g/m^2 constraint.

Table 4.10. F Analysis by IC for ML-107A Glasses

Glass	Target	Measured	% Difference
ML-107A-40	5.96	5.44	8.7
ML-107A-42	6.26	5.58	10.9
ML-107A-44	6.56	5.99	8.7

Table 4.11. PCT results for ML-107A- Glasses at 40, 42, and 44 mass% Loadings

Glass ID	r_B (g/m^2)	r_{Li} (g/m^2)	r_{Na} (g/m^2)	pH
ML-107A-40 Q	0.1206	0.1875	0.1262	10.30
ML-107A-42 Q	0.1111	0.1801	0.1185	10.27
ML-107A-44 Q	0.1015	0.1757	0.1097	10.24

4.3 Alternative Scoping Studies for Glass-Forming Regions

Crystallization and/or amorphous phase separation of the glass upon quenching has limited waste loading of previous frits developed by Musick et al. (2000) for Run 78 calcine and is expected to limit waste loading for Blend calcine. To supplement the studies described in section 4.2, a second set of frits was developed and tested in an attempt to find a glass-forming region that will accept higher waste loadings than were found when developing frits ML-102 through -108 without crystallization upon cooling. Frit composition and waste loading were varied to identify a glass-forming region that accommodates higher waste loading of the Blend calcine waste. The compositions of Frits 1 through 20 of Table 4.12 were selected using preliminary models developed from past data. However, because of the goal to increase waste loading, the resulting glass compositions at the higher waste loadings were outside the model validity range. Glass-property predictions for glasses outside of the model's composition region (extrapolation) can have significant error. Thus, many of these frits may not produce a glass that satisfies all of the processing and product constraints (refer to Table 3.2).

The primary intent of this study was to evaluate the impacts of frit compositional changes on the capability to minimize (or eliminate) devitrification in the final product. The impacts to the viscosity, T_L, and r_i of the resulting glasses were not evaluated. Each of the glasses based on frit compositions listed in Table 6.14 were fabricated in succession using standard melting procedures as discussed in the following section.

Table 4.12. Frit Composition, Waste Loading, and Observations of the Quenched Glass after Melting

ID	B_2O_3	La_2O_3	Li_2O	Na_2O	SiO_2	Waste Loading	Observations
	Mass%					Mass%	
1	30.00	0.00	10.00	0.00	60.00	46.00	SPS
2	30.00	0.00	0.00	10.00	60.00	46.00	MPS
3	0.00	0.00	15.00	20.00	65.00	46.00	MPS
4	40.00	0.00	0.00	10.00	50.00	46.00	MPS
5	50.00	0.00	0.00	0.00	50.00	46.00	MPS
6	35.00	0.00	10.00	0.00	55.00	46.00	SPS
7	28.00	0.00	9.00	6.00	57.00	46.00	MPS
8	30.00	10.00	10.00	0.00	50.00	46.00	HG
10	0.00	0.00	0.00	0.00	100.00	66.00	CG
11	30.00	10.00	5.00	0.00	55.00	46.00	MPS
12	20.00	10.00	7.75	7.25	55.00	46.00	SPS
13	5.00	0.00	10.00	0.00	85.00	63.00	CG
14	25.00	9.00	5.00	5.00	56.00	46.00	SPS
16	15.00	9.00	10.00	10.00	56.00	46.00	SPS
19	10.00	60.00	0.00	0.00	30.00	40.00	CG
20	10.00	55.00	0.00	0.00	35.00	50.00	CG

SPS=slightly phase separated [(a)] glass, MPS= massively phase separated glass, HG= homogenous glass and no phase separation, and CG= crystals in the quenched glass but no phase separation.

4.3.1 Glass Fabrication Process

Blend calcine waste mix was weighted to a hundredth of a gram using the chemical compounds and concentrations shown in Table 4.13, with the exception of replacing B_2O_3 with H_3BO_3. The batch was then placed in an agate milling chamber and mixed for 8 min to homogenize the waste mix. The measured loss on ignition (LOI) for waste heat treated at 1150°C for 2 h in an alumina crucible was 9.24 mass%. A second LOI measurement of the Blend calcine waste was done using a differential thermal analysis/thermogravimetric analysis (DTA/TGA). Results of the DTA/TGA measurement of LOI was 8.88 mass% at a temperature of 1200°C. This Blend calcine batch was added to each of the glass batches as the waste component.

(a) Note that phase separation refers to crystallization of sub-micron size particles.

Table 4.13. Blend Calcine Waste Mix Chemical Compounds and Concentrations

Compounds	Mass%
Al2O3	32.49
B2O3*	2.33
CaO	2.96
CaCO3	2.58
CaF2	31.04
CaSO4	3.03
Ca3(PO4)2	0.44
CoCO3	0.06
CsCl	0.31
Fe2O3	0.58
K2SO4	1.02
MgO	0.84
MnO	0.03
NaNO3	5.70
Na2CO3	1.61
NaCl	0.07
NiO	0.74
SnO2	0.20
SrO	0.25
ZrO2	13.73
Total	100.00

Glasses were batched by weighing out the frit components using oxides, carbonates, and boric acid, then adding the Blend calcine waste mix necessary for the desired waste loading. Chemicals were weighted out to a hundredth of a gram. The batch was then homogenized in an agate milling chamber for 4 min. Glasses were batched at various waste-loading levels of Blend calcine waste (as shown in Table 6.14). Melting was performed in a platinum crucible covered by a lid. Each glass was melted for 1 h and quenched, ground in a tungsten carbide mill, and remelted for 1 h and quenched. Observations about the quenched glass were made following each melt.

Frit composition, waste loading, and observations of the quenched glass are shown in Table 4.12. Nearly all of the glasses phase separated upon quenching after the first melt. Although there was slight to significant improvement observed following the second melt, all but a few glasses phase separated at either T_M or most commonly upon quenching (as indicated by a visually homogenous region at the quench plate glass interface). The quench rate of the glasses was similar to the cooling curve shown in

Figure 4-4. No additional testing was performed for glasses that phase separated upon quenching. Of the glasses that did not phase separate, only Frit 8 produced a visually homogenous glass at a waste loading of 46 mass% Blend calcine waste. For this reason, Frit 8 was selected for further testing.

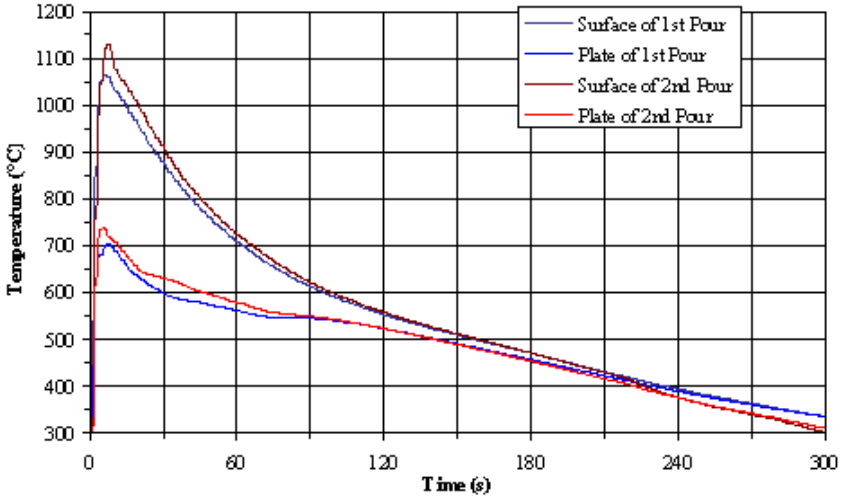

Figure 4-4. Cooling Rate of Melt at 1150°C Poured onto a Stainless Steel Quench Plate

4.3.2 Further Testing of Frit 8

Opalescence Temperature

Opalescence temperature was measured with hot-stage optical microscopy. A sample of Frit 8-40% waste loading (WL) was loaded into a small platinum crucible and heated from room temperature to a starting temperature of 500°C. The temperature was periodically raised in approximately 5-20°C increments to find the temperature at which phase separation disappeared visually. Up to temperatures of 800°C, the sample was visually cloudy, indicating phase separation. At 805°C, the glass became clear under the microscope at a magnification of 20X. An estimate of 803°C was determined to be the opalescence temperature. Opalescence is most likely the formation of CaF_2 or other F-containing phases. The opalescence temperature should not be considered as the T_L of the glass. Some crystals remained in the sample at temperatures above 805°C. These crystals are thought to be baddelleyite (ZrO_2) based on visual observations of morphology. The growth and dissolution rates of baddelleyite are expected to be significantly lower than those of CaF_2, based on previous experience.

Melt Time Necessary at 1150°C to Achieve a Homogenous Quenched Glass

A series of melt times was chosen to estimate the time required to achieve a homogeneous quenched glass when starting from a batch. A portion of 50 g from a 200-g batch was added to each platinum crucible and covered with a lid. Each crucible was put into the furnace at 1150°C for times of ½, 1, and 2 h. They were then removed from the furnace and allowed to air cool. The samples were then examined visually and optically.

At ½ h, the sample showed slight phase separation at the bottom surface. At 1 and 2 h, the samples appeared visually homogeneous and free of phase separation and undissolved materials. The time to homogeneity for Frit 8-40%WL glass was bracketed between ½ and 1 h. These samples were not examined by XRD to confirm the results.

Crystallization During CCC Heat Treatment

Frit 8-40 and -45%WL glasses were subjected to CCC heat treatment. Approximately 20 g of glass were placed into a Platinum-5% gold crucible and put into a furnace at 1150°C for 1 h. It was then cooled according to the schedule shown in Table 3.1.

Samples were examined visually and by XRD. The samples were visually crystallized. CaF_2 and ZrO_2 were identified by XRD with Frit 8-40%WL having 1.89% CaF_2 and 0.56% ZrO_2 and Frit 8-45%WL having 2.08% CaF_2 and 2.49% ZrO_2. Concentrations of the crystalline phases are only semi-quantitative.

Summary of Testing of Frit 8

Frit 8 was developed to determine if it is possible to achieve higher levels of waste loading than those achieved with Frits 102-108. Frit 8 is capable of waste loadings of up to 45 mass% Blend calcine waste without exhibiting crystallization or phase separating upon quenching. Additionally, only limited crystallization occurred during CCC heat treatment.

4.4 Candidate Frit: ML-107

Based on the results of the tests using the estimated Blend calcine composition, ML-107 was chosen as the primary candidate frit for supporting the pilot-scale melter demonstration run. Given that the

"visual homogeneity boundary" for this particular frit was defined to be between 42 and 44 mass%, a targeted loading of 40 mass% was selected. This targeted loading should allow for minor variations in loading during the melter run without having a significant impact on the homogeneity of the final product. Although the Blend calcine composition had slightly higher F concentrations, the targeted waste loading is slightly higher than that used for the Run 78 calcine. This increase in waste loading is primarily caused by relaxing the self-imposed 2 vol% crystallization constraint after CCC.

Before recommending Frit ML-107 for the melter demonstration, this glass was refabricated and fully characterized to ensure that it meets the targeted properties agreed to by the technical team. Properties to be evaluated (or confirmed or re-evaluated) include:

- Homogeneity of quenched glass (visual and XRD)
- Homogeneity of CCC glass (visual, XRD, scanning electron microscope/energy dispersive spectroscopy [SEM/EDS])
- Opalescence temperature
- PCT on quenched and CCC glasses
- T_L
- η
- Electrical conductivity
- Devitrification/Remelt Potential
- Density
- Glass Transition Temperature
- Melt Behavior.

Four batches were made with Frit ML-107 with a Blend calcine waste loading of 40 mass%. Two batches of ML-107A-40 glass (targeted 400 g of glass) were fabricated using oxides, carbonates, and boric acid precursors according to standard procedures. Two additional batches were made using oxides, carbonates, and boric acid for the frit additives and Blend calcine simulant as the waste. Blend calcine simulant waste was batched following the procedure disscused in section 4.3.1. One batch was produced using laboratory chemicals (MaxWL-107-40%WL), and the second was made using chemicals selected for use in the upcoming melter run (MaxWL-107-40%WL-MR). The glasses were fabricated at different laboratories to ensure reproducibility. These glasses were melted for 1 h at 1150°C in a covered Pt/Rh crucible, quenched on a steel plate, ground in a WC mill, remelted for 1 h, and quenched on a steel plate. The resulting pour patty was then used as stock for obtaining samples for the various property measurements.

4.4.1 Homogeneity

All of the glasses were visually homogeneous upon quenching (see Table 4.14). A representative sample of each as-fabricated ML-107A-40 glass was submitted for XRD to confirm visual observations of homogeneity (i.e., no crystallization). Both glasses were homogeneous based on the XRD results. As an example, the XRD pattern for ML-107A-40-1 is shown in Figure 4-5[(a)] The XRD pattern shows the characteristic amorphous hump indicative of a homogeneous (non-crystalline) product. That is, if crystalline material were present in the sample in sufficient quantity, well-defined or distinct peaks would be observed that could be used to identify the phase. It should be noted that the X-ray diffractometer used in this study has a detection limit of approximately 1.0 vol% in glass. Undissolved solids and/or crystallization present below this limit remain undetected by the XRD unit.

Table 4.14. Visual and XRD Results for the Frit 107 Glass with 40 mass% Blend Calcine Waste

Glass	Visual	XRD
ML-107A-40-1	Homogeneous	Amorphous
ML-107A-40-2	Homogeneous	Amorphous
MaxWL107-40%WL	Homogeneous	NA
MaxWL107-40%WL-MR	Homogeneous	NA

4.4.2 Effect of CCC

Approximately 30 g of ML-107A-40-1 and -2 were each placed in a platinum/rhodium crucible, heated to 1150°C, held at temperature for 1 h, and then cooled according to the CCC profile.[(b)] As discussed in an earlier section, the volume-percent devitrification will not be a limiting factor in terms of waste loading as long as there was not a negative impact on durability (ri $\leq$ 1 g/m^2).

Visual observations of ML-107A-40-1 and -2 after CCC indicated < 2 vol% crystallization on each of the heat-treated glasses (although crystallization is not a constraint). Crystallinity was confined primarily to the surface of each glass melt. Figure 4-6 and Figure 4-7 show a representative photograph and an optical micrograph, respectively, of ML-107A-40-1. Figure 4-8 and Figure 4-9 show a representative photograph and an optical micrograph of ML-107A-40-2, respectively.

(a) XRD patterns for both ML-107A-40 glasses are characterized by an amorphous hump indicative of a glassy, homogeneous product within the detection limits of the X-ray diffractometer. Note that the absence of well-defined peaks does not provide an indication of chemical homogeneity, but simply the absence of crystalline material.
(b) The durability and homogeneity of the CCC glasses were measured for comparison to their quenched counterpart glasses.

Approximately 20 g of MaxWL107-40%WL and MaxWL-107-40%WLMR glasses were loaded into a platinum/gold crucible and heat treated according to the CCC schedule as given in Table 3.1. The heat-treated samples were examined by optical microscopy and XRD to determine the phases present and their concentrations.

The CCC sample of MaxWL107-40%WL glass was cross sectioned and examined by optical microscopy using reflected light. As Figure 4-10 shows, the sample contains 1–2 vol% of crystalline material.

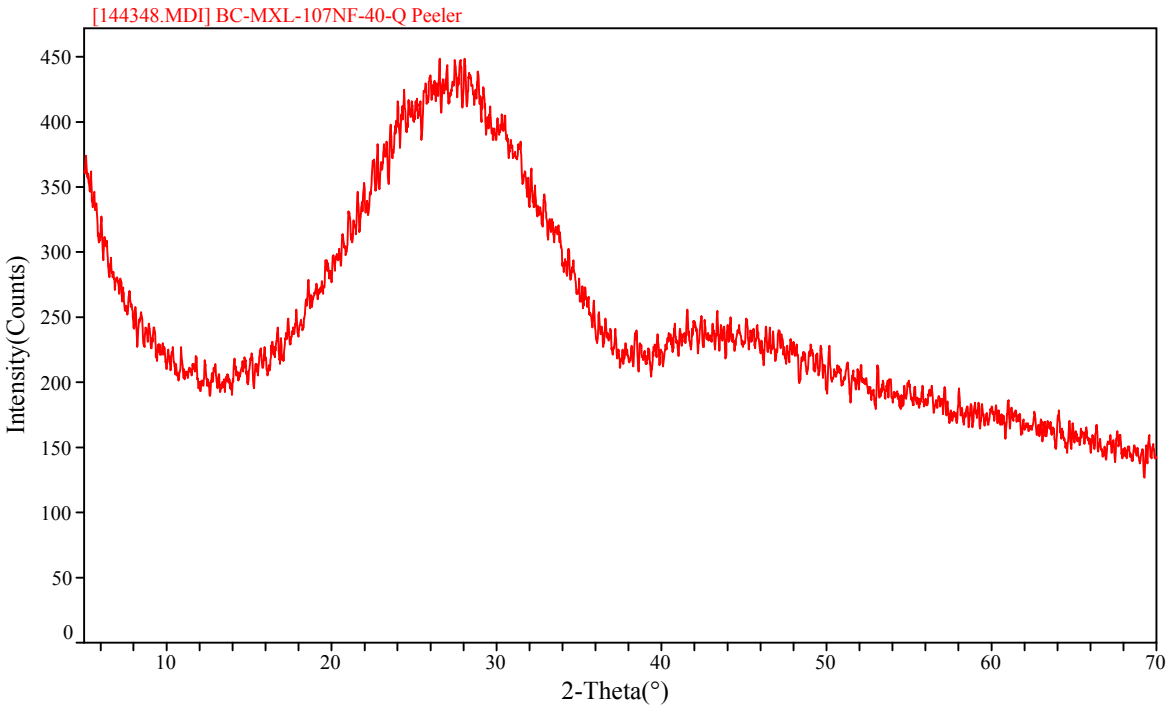

Figure 4-5. XRD Results of ML-107A-40-1 (as-fabricated)

Figure 4-6. Photo of ML-107A-40-1 After CCC

Figure 4-7. Optical Micrograph of ML-107A-40-1 After CCC (8x)

Figure 4-8. Photo of ML-107A-40-2 After CCC

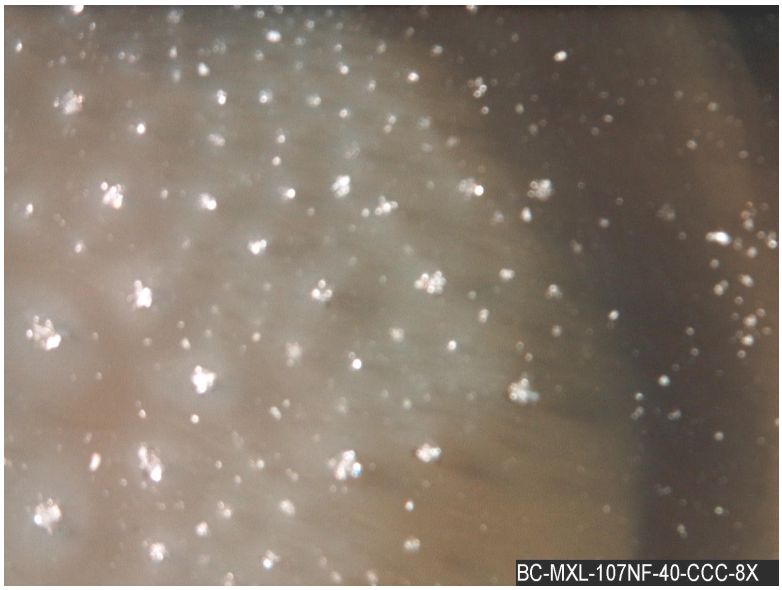

Figure 4-9. Optical Micrograph of ML-107A-40-2 after CCC (8x)

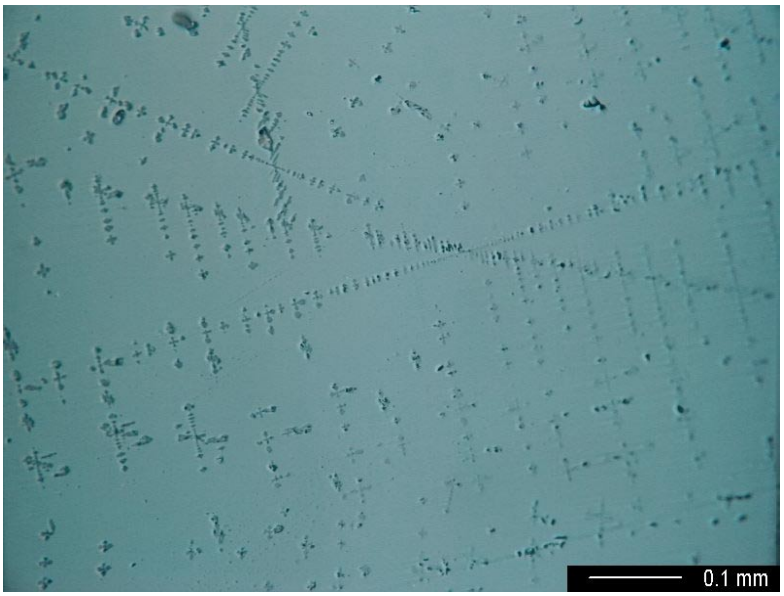

Figure 4-10. Optical Micrograph of Cross-Section of MaxWL-107-40%WL After CCC Using Reflected Light

XRD patterns of ML-107A-40-1 and ML-107A-40-2 after CCC are shown in Figure 4-11 and Figure 4-12, respectively. Fluorite (CaF_2) and lithium aluminum silicate ($LiAlSi_2O_8$) were identified in ML-107A-40-1 (Figure 4-11) while CaF_2 was identified in ML-107A-40-2 (Figure 4-12). XRD results of MaxWL-107-40%WL are shown in Table 4.15. Total crystallinity is below 2 mass% in each of the three samples, and the major crystalline phase is CaF_2. Two minor phases were identified at detection or near detection limits for different samples, and the third contained no minor crystalline phases. The identification of the minor phases should be considered suspect because of the lack of peaks in the XRD scans that would more positively identify the crystalline structure.

Table 4.15. Semi-Quantitative Results of MaxWL 107-40 as Measured by XRD

MaxWL107-40%WL	Weight Percent
CaF_2	1.14
ZrO_2	0.22
Amorphous	98.64
Total	100

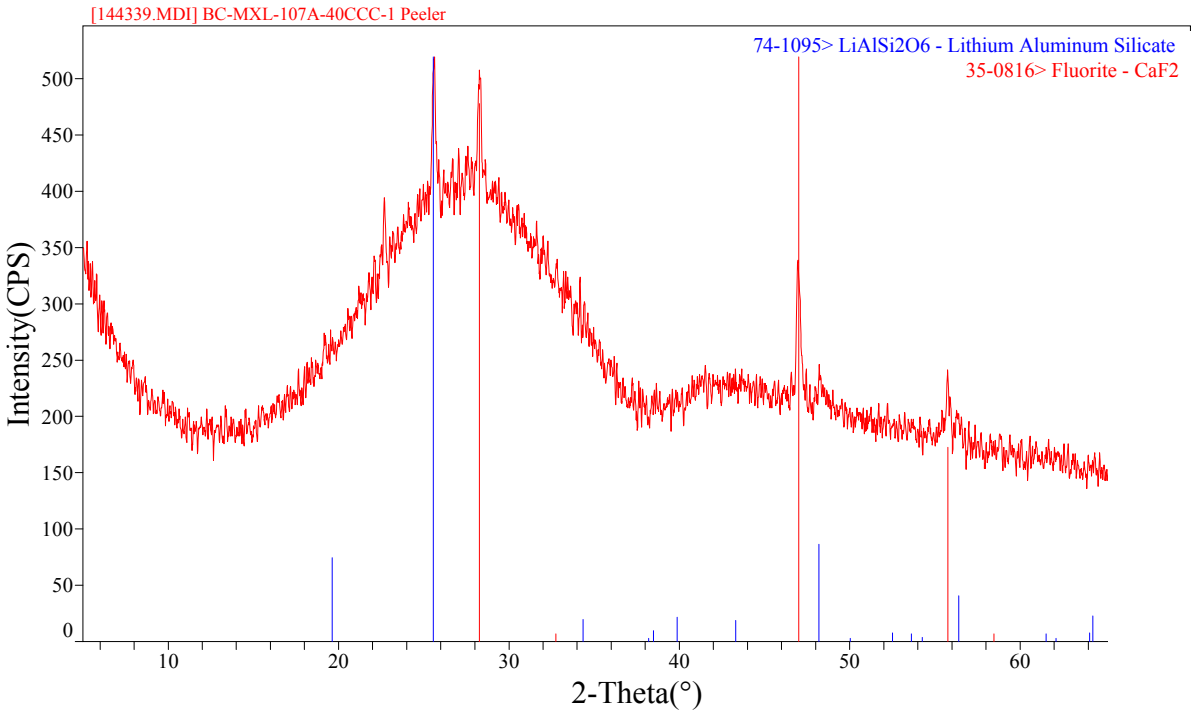

Figure 4-11. XRD Pattern for ML-107A-40-1 CCC

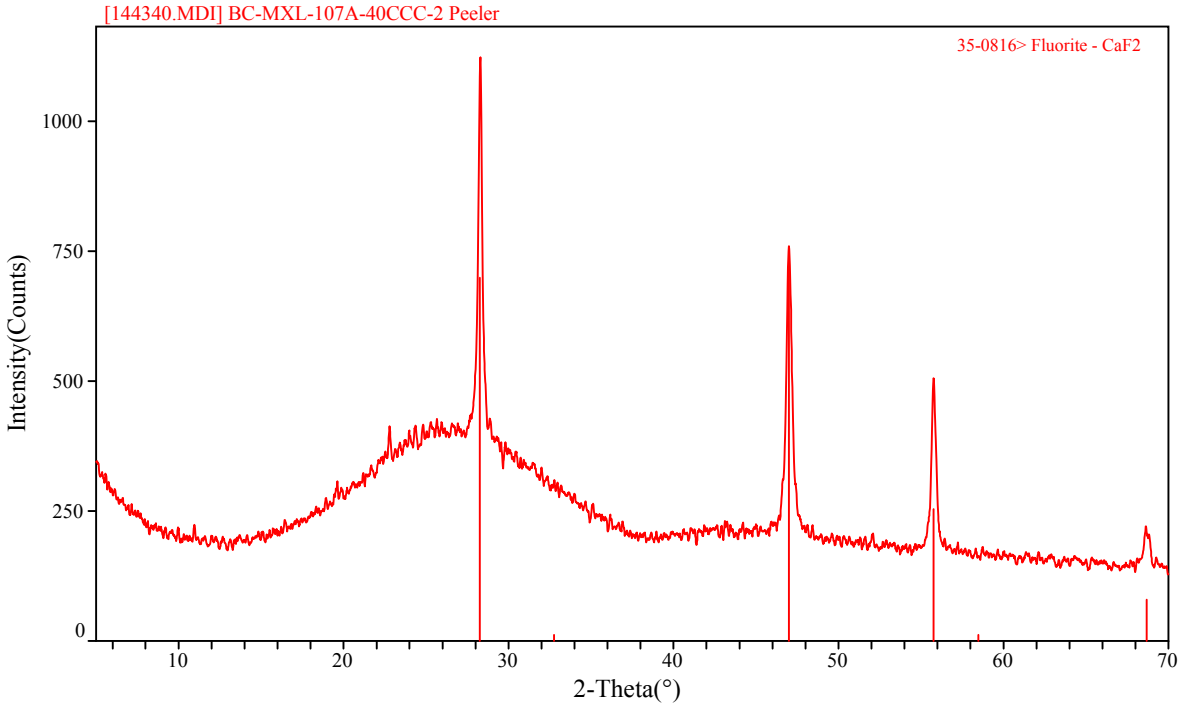

Figure 4-12. XRD Pattern for ML-107-40-2 CCC

SEM with EDS was also used to evaluate each glass after CCC. Figure 4-13 and Figure 4-14 show micrographs of ML-107A-40-2 CCC with islands of crystals isolated in a glass matrix. EDS, shown in Figure 3-1 analysis, indicated that the crystals are enriched in Ca (relative to the glass baseline spectra). Although F is not detected in the spectra, the presence of Ca matches very well to the XRD pattern for this glass (shown in Figure 4-12), which identified CaF_2.

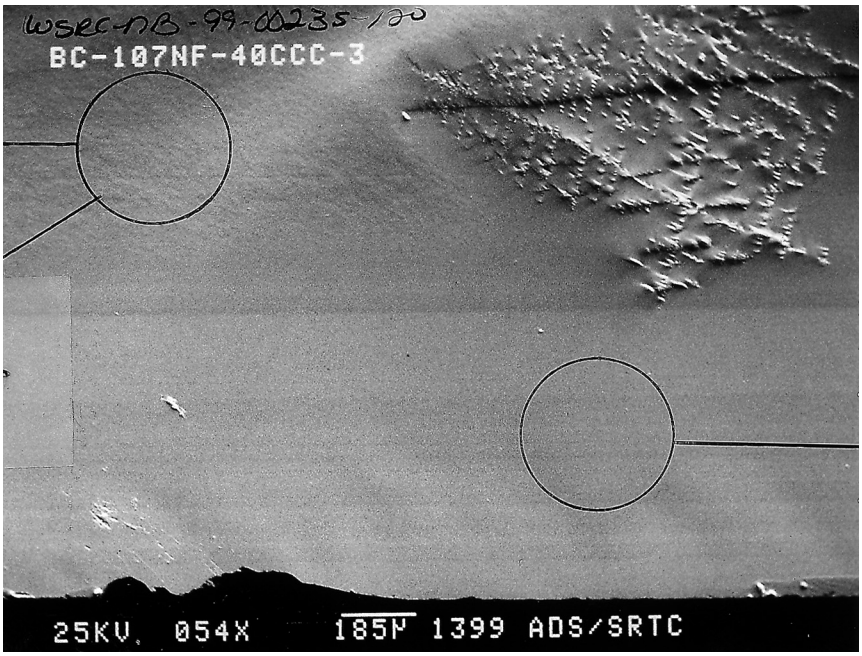

Figure 4-13. SEM Micrograph of ML-107A-40-2 CCC (54x)

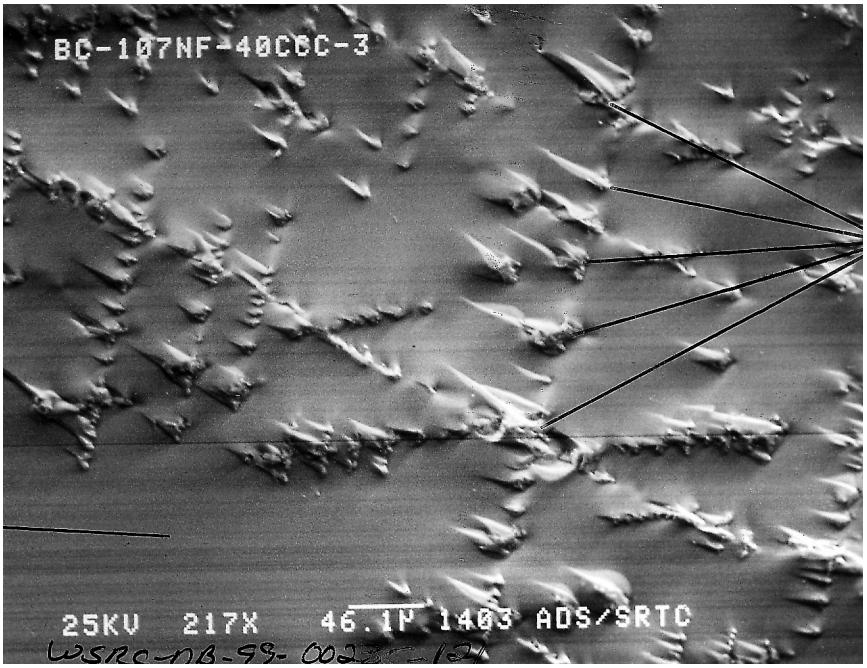

Figure 4-14. SEM Micrograph of ML-107A-40-2 CCC (217x)

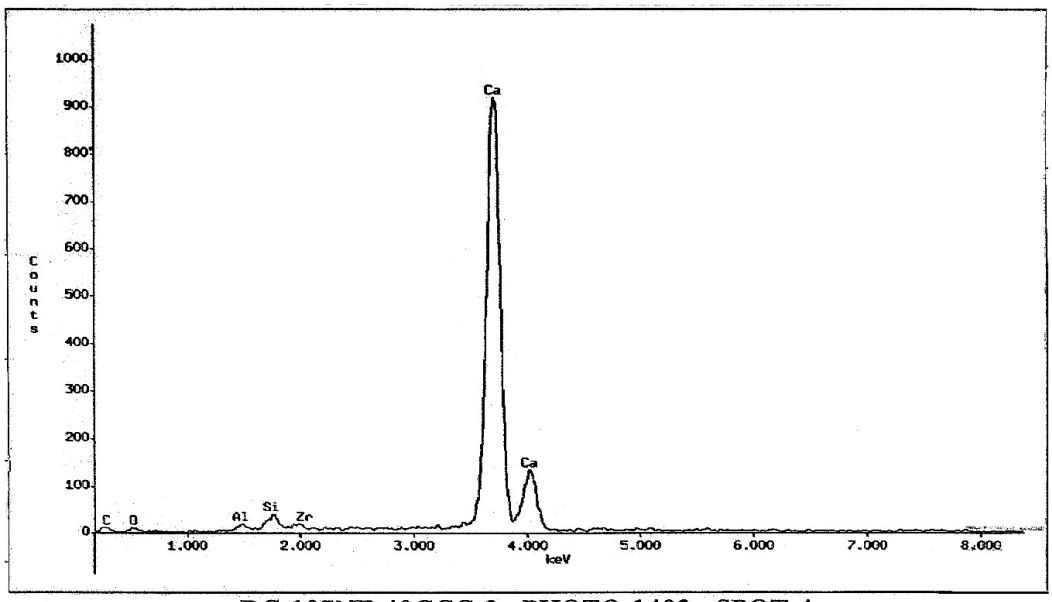

Figure 4-15. EDS Spectra Ca-Rich Phase in ML-107A-40-2 CCC

4.4.3 Opalescence Temperature

Opalescence temperature was measured with hot-stage optical microscopy using the procedure stated in section 4.3.2. An estimate of 773°C was determined to be the opalescence temperature. CaF_2 is most likely the separated phase. The opalescence temperature should not be considered the T_L of the glass. Some crystals remained in the sample at temperatures above 775°C. These crystals are presumed to be baddelleyite (ZrO_2), based on visual observations of morphology. The optical microscope has an open-top crucible for observation purposes and as a result, it subjects the sample to high volatility rates at temperatures greater than 800°C (for this particular glass). For this reason, the T_L of the glass was not measured by this method.

4.4.4 PCT on Quenched and CCC Glasses

PCT was performed to assess the durability of quenched and CCC samples of both ML-107A-40-1 and ML-107A-40-2 glasses. The r_i values, normalized to target compositions, are reported in Table 4.16. All r_i values are well below those reported for the EA glass (see Table 4.3) as well as the conservative constraint of 1 g/m^2 being used in this study.

4.4.5 Liquidus Temperature

A T_L constraint for these glasses has been set at T_M – 100°C. To determine if T_L was below 1050°C, 5 g of glass were placed in a platinum/rhodium crucible, which was then placed into a preheated furnace at 1050°C. The glass was held at temperature for 24 h and then removed from the furnace. The glass was allowed to cool to room temperature while in the crucible.[(a)] The sample was then analyzed for crystal formation using visual inspection and OM.[(b)] The T_L was only determined on quenched glasses that were amorphous. Visual observations were confirmed by XRD analysis.

Table 4.16. PCT Results of ML-107A-40-1 and ML-107A-40-2 Glasses

Glass ID	r_B (g/m^2)	r_{Li} (g/m^2)	r_{Na} (g/m^2)	pH
ML-107A-40-1 Q	0.0349	0.1011	0.1227	10.40
ML-107A-40-1 CCC	0.0552	0.1285	0.1024	10.44
ML-107A-40-2 Q	0.0280	0.0925	0.1040	10.32
ML-107A-40-2 CCC	0.0512	0.1273	0.0910	10.44

No crystallization was observed by either visual observations or OM evaluation, indicating that the T_L < 1050°C. A photograph of the ML-107A-40-2 glass is shown in Figure 4-16.

A gradient furnace method was also used to measure the T_L of MaxWL-107-40%WL. The T_L was observed to be approximately 1004°C at the bottom surface of the sample and 960°C at the top surface of the sample. A trace amount of crystals in the bulk of the glass, which appeared to be dissolving, appeared to travel into hotter regions of the sample (>1004°C) than either the top or bottom of the sample. A conservative estimate of T_L would be 1004°C, which is consistent with visual and OM results previously discussed.

XRD patterns of ML-107A-40-1 and ML-107A-40-2 heat treated at 1050°C for 24 h confirmed visual observations of homogeneity (see Figure 4-17 and Figure 4-19,

Figure 4-16. ML-107A-40-2 After 24-H Isothermal Hold at 1050°C

(a) The procedure used was similar to Method B of PNNL procedure GDL-LQT, "Standard Test Methods for Determining the T_L of Waste Glasses and Simulated Waste Glasses."
(b) Optical microscopy was performed at 108x magnification.

respectively). The XRD patterns show the characteristic amorphous hump indicative of a homogeneous (non-crystalline) product (at the detection limit of the diffractometer).

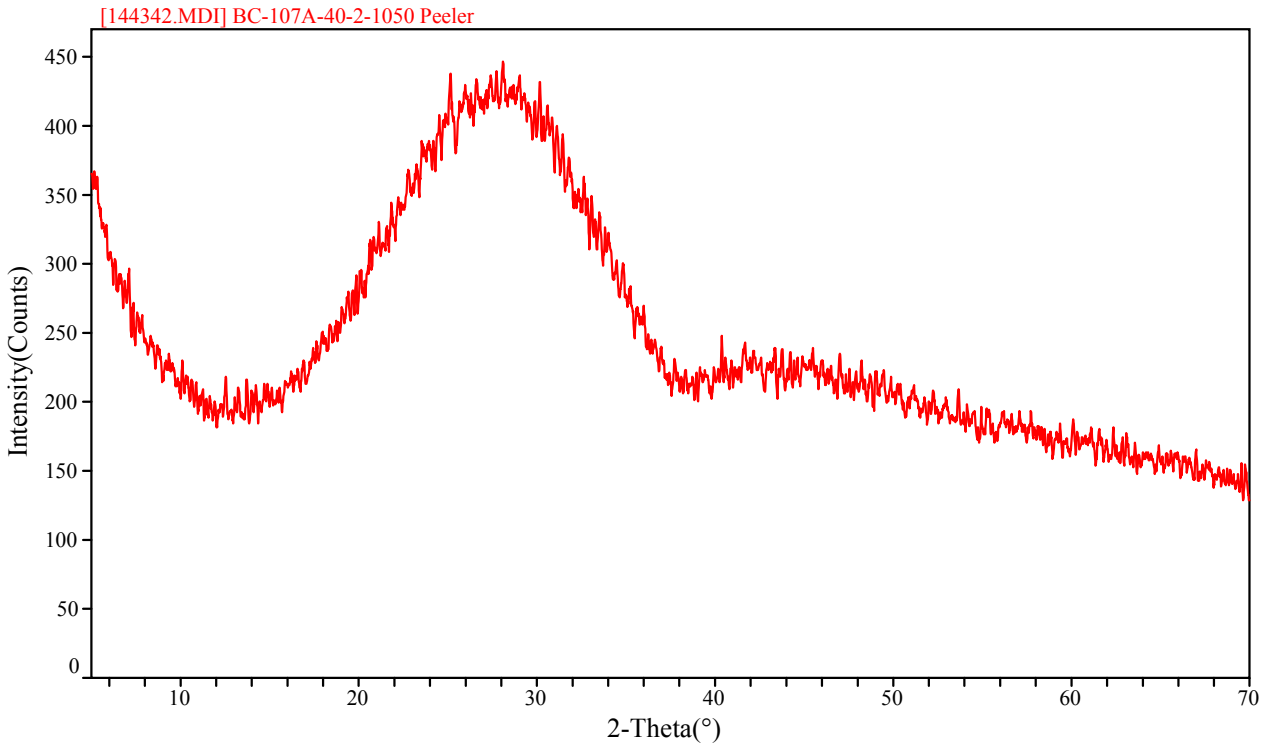

Figure 4-17. XRD Pattern for ML-107A-40-1 after 24 H at 1050°C

4.4.6 Viscosity / Electrical Conductivity

Table 4.17, Table 4.18, and Table 4.19 show the viscosity and electrical-conductivity for glasses MaxWL-107-40%WL and MaxWL-107-40%WL-MR. Formulation efforts of these glasses were aimed at producing a glass that melts at 1125 ± 25°C. Figure 4-18 shows the viscosity-temperature relationship of these glasses. The 2 Pa·s limit is crossed at roughly 1070°C for MaxWL-107-40%WL and at roughly 1050°C for MaxWL-107-40%WL-MR. Electrical-conductivity measurements are acceptable for processing in a joule-heated melter from 950°C up to at least the highest measured temperature of 1150°C. Comparison of the measured viscosity and electrical conductivity of the two glasses shows good agreement, considering the different sources and purity of the chemicals.

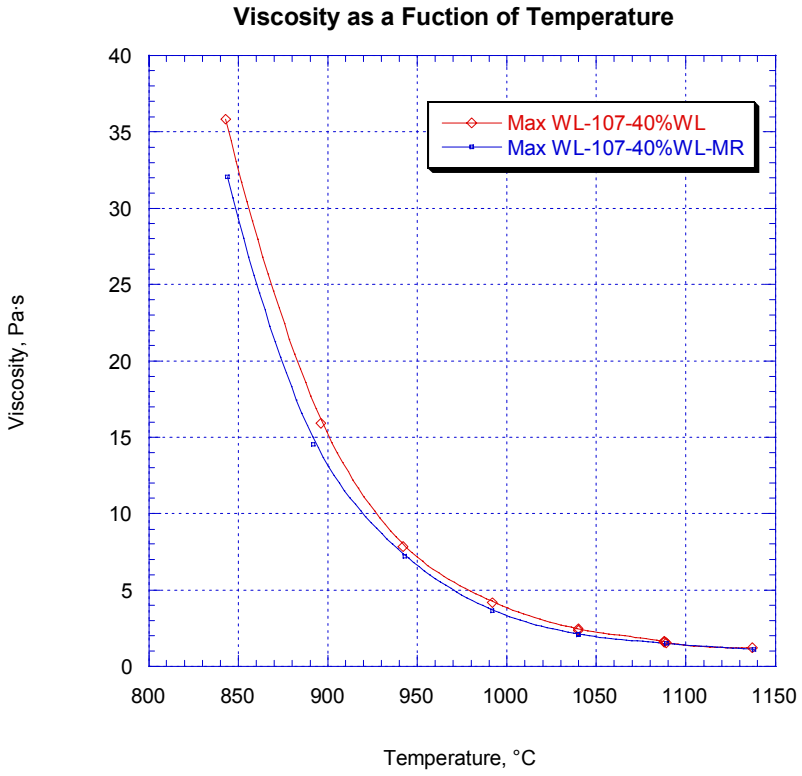

Figure 4-18. Viscosity as a Function of Temperature for Max WL-107-40%WL and Max WL-107-40%WL-MR Glasses.

To maintain high F solubility in glass as waste loading is increased, the alkali concentration is increased and SiO_2 is decreased, resulting in a decrease in viscosity. Because of the composition region needed to keep F soluble, η will become a limiting factor on waste loading if the T_M is to be maintained at 1125 ± 25°C.

The glass-transition temperature and the softening temperature of MaxWL-107-40%WL were measured using a dual-rod dilatometer. Figure 4-20 shows the expansion versus temperature and the fitted lines used to determine T_g and T_s. The estimated T_g is 419°C, and the T_s is 492°C.

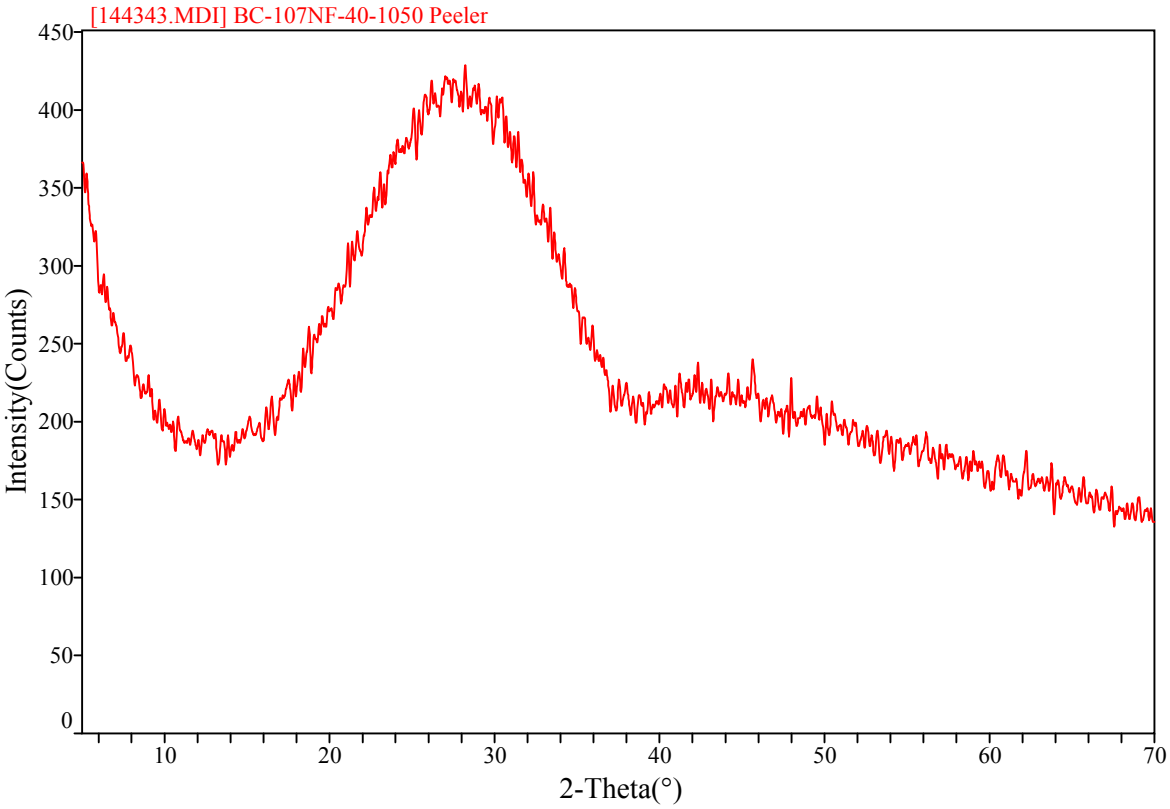

Figure 4-19. XRD Pattern for ML-107-40-2 after 24 H at 1050°C

Table 4.17. Viscosity Measurements

MaxWL-107-40%WL			MaxWL-107-40%WL-MR		
Temperature, °C	**η, Pa·s**	**Ln (η), Pa·s**	**Temperature, °C**	**η, Pa·s**	**Ln (η), Pa·s**
1088	1.630	0.489	1089	1.479	0.391
1040	2.465	0.902	1040	2.060	0.723
992	4.193	1.433	992	3.637	1.291
1040	2.364	0.860	1040	2.102	0.743
1088	1.573	0.453	1089	1.494	0.401
1137	1.208	0.189	1138	1.123	0.116
1089	1.548	0.437	1089	1.491	0.399
942	7.847	2.060	943	7.209	1.975
896	15.939	2.769	892	14.533	2.676
843	35.846	3.579	844	32.058	3.468

Table 4.18. Electrical Conductivity Measurements of MaxWL-107-40%WL

Temperature °C	Temperature °K	1/K*10000	Resistance ohms	Resistance corrected*	Conductivity S/m
1144	1417	7.057	0.85	0.837	36.68
1045	1318	7.587	1.218	1.206	25.46
946	1219	8.203	1.99	1.98	15.5
846	1119	8.937	3.963	3.955	7.76

Table 4.19. Electrical Conductivity Measurements of MaxWL-107-40%WL-MR

Temperature °C	Temperature °K	1/K*10000	Resistance ohms	Resistance corrected*	Conductivity S/m
1144	1417	7.057	0.851	0.838	36.65
1046	1319	7.584	1.215	1.204	25.51
946	1219	8.203	1.990	1.980	15.50
846	1119	8.937	3.958	3.950	7.77

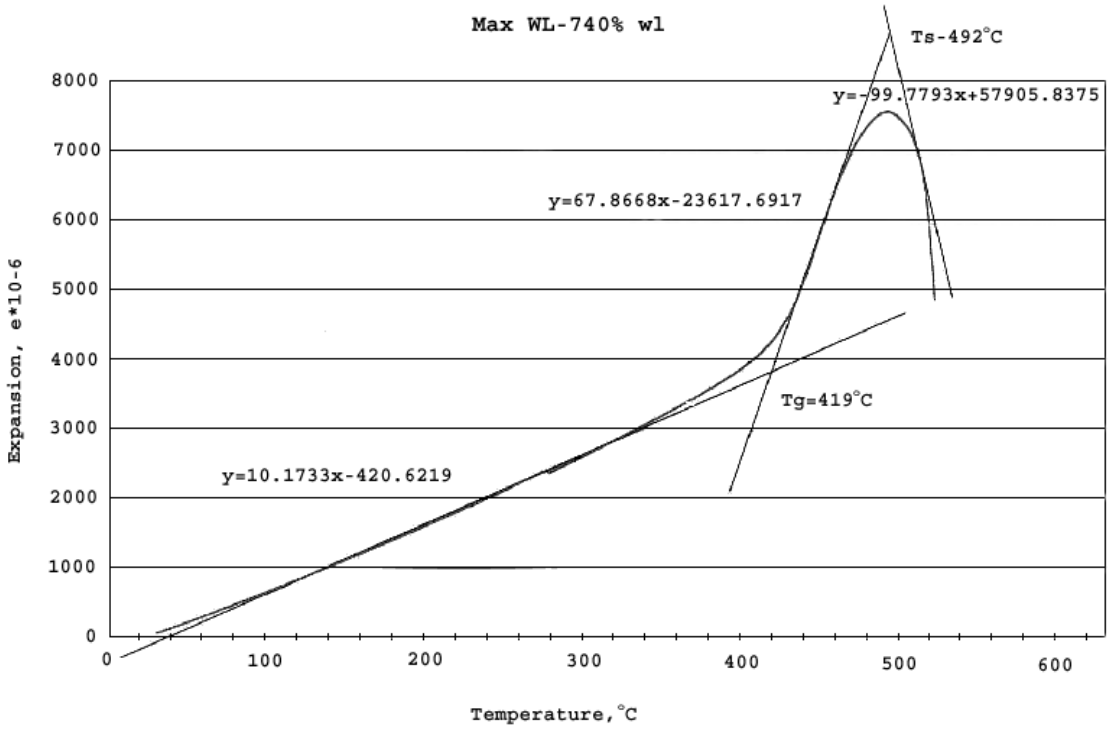

Figure 4-20. Plot of Expansion Versus Temperature for Max WL-107 40mass% WL Glass

4.4.7 Glass Density

In an attempt to fully characterize MaxWL-107-40%WL glasses, density was measured using a gas pycnometer. The measured density of MaxWL-107-40%WL was 2.7223 g/cm^3 with a standard deviation of 0.0007 g/cm^3 and MaxWL-7-40%WL-MR was 2.7256 g/cm^3 with a standard deviation of 0.0007 g/cm^3. These values are similar to those for DWPF and WVDP glasses despite obvious compositional differences in this glass.

4.4.8 Devitrification/Remelt Potential

The melter pour spout is essentially a water-cooled tube which when inactive holds a glass plug (e.g., cooled to increase η, resulting in a glass plug). Under idling or non-pour conditions, a thermal gradient will exist down the length of the drain tube from the nominal operating temperature (near the molten glass pool) to a few hundred degrees. Given this thermal gradient, the glass within the drain tube is likely to devitrify. To reduce the risk of plugging the drain tube with a devitrified product, an assessment of the devitrification and remelt potential is warranted. Even if devitrification does occur, the question then

remains: When the drain tube is heated to initiate pouring, will the crystals remelt, or is there sufficient (a continuous) glass phase to avoid pluggage?

The potential for ML-107A-40 to devitrify was assessed by heat treating both glasses at 750°C for 48 h. Although 750°C may not be the optimal temperature of devitrification, based on experience with this glass, this temperature will allow for ample devitrification to occur. The objective of this test is to assess the devitrification potential of this glass as the melter is idled (e.g., non-pour operation).

As-fabricated samples of ML-107A-40-1 and ML-107A-40-2 were heat treated at 750°C for 48 h. As expected, both samples were highly devitrified (estimated to be > 90 vol%). Visual observations of high crystal content were confirmed by SEM/EDS and XRD analyses. XRD results of ML-107A-40-1 and ML-107-40A-2 indicated that both samples contain $LiAlSi_2O_6$, CaF_2, and ZrO_2 (see Figure 4-21 and Figure 4-22).

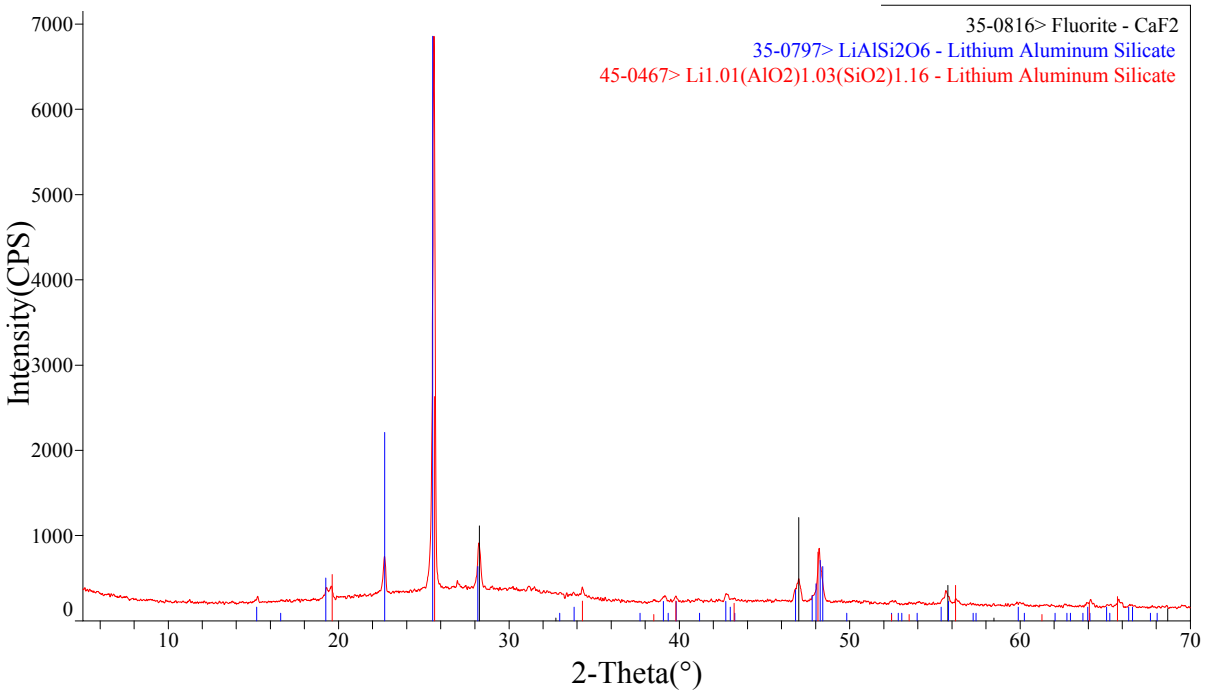

Figure 4-21. XRD Pattern for ML-107A-40-1 after 48 H at 750°C

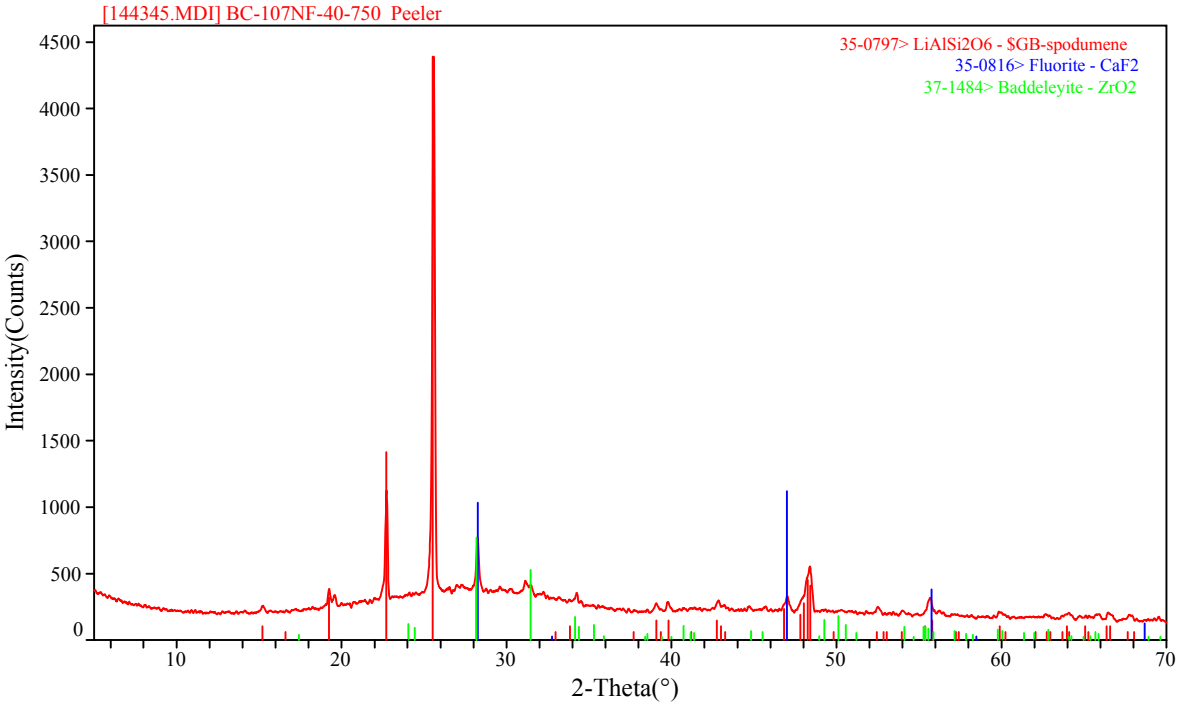

Figure 4-22. XRD Pattern for ML-107-40-2 after 48 H at 750°C

SEM analysis of ML-107A-40-2 (48 h at 750°C) also confirmed visual observations of a highly devitrified sample. Figure 4-23 and Figure 4-24 show the high percentage of devitrification observed on the surface of the glass.

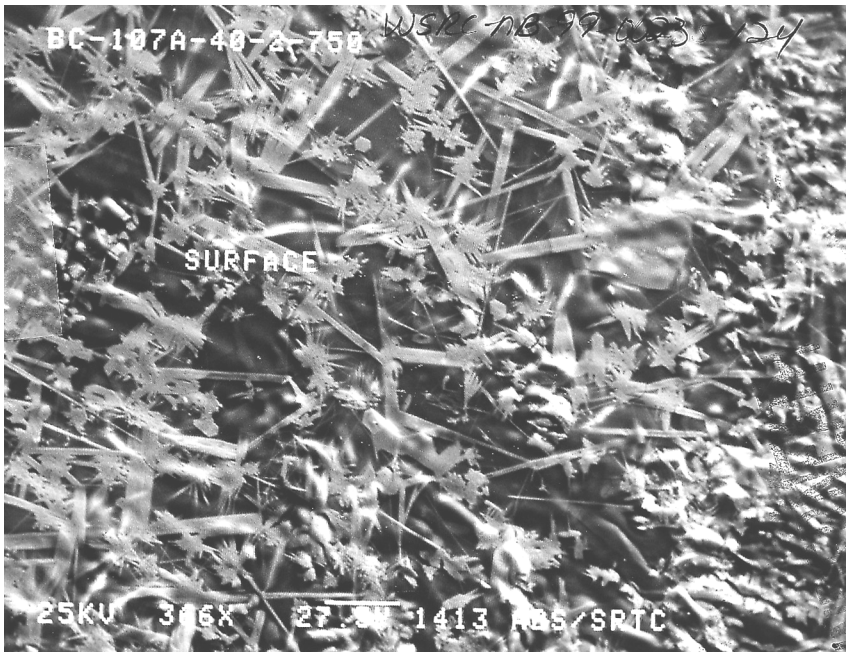

Figure 4-23. SEM Micrograph of ML-107A-40-2 After 48 H at 750°C (366x)

Figure 4-24. SEM Micrograph of ML-107A-40-2 After 48 H at 750°C (920x)

To assess the potential to remelt these crystals, two samples of each glass were placed in Pt/Au crucibles (four crucibles total) and inserted into a preheated furnace at 1000°C. Samples of each glass were pulled after 1 and 2 h then allowed to air cool. All four samples were visually homogeneous with no apparent crystallinity. XRD patterns for ML-107A-40-2 identified ZrO_2 in both the 1- and 2-h remelts are in Figure 4-25 and Figure 4-26. Based on the intensity of the ZrO_2 peaks, the quantity of ZrO_2 is very limited 2-5 vol%. Even though ZrO_2 exists in the remelted samples, its fraction is insufficient to plug the drain tube (i.e., a continuous glass phase will exist that should flush the drain tube). These results suggest that even if massive devitrification does occur within the drain tube, once heat is applied and temperatures reach 1000°C, a continuous glass phase should form (in less than 1 h), and pouring should not be impeded. Again, the assumptions for this test are that 750°C is the optimal devitrification temperature, and the drain tube is capable of heating to 1000°C or higher.

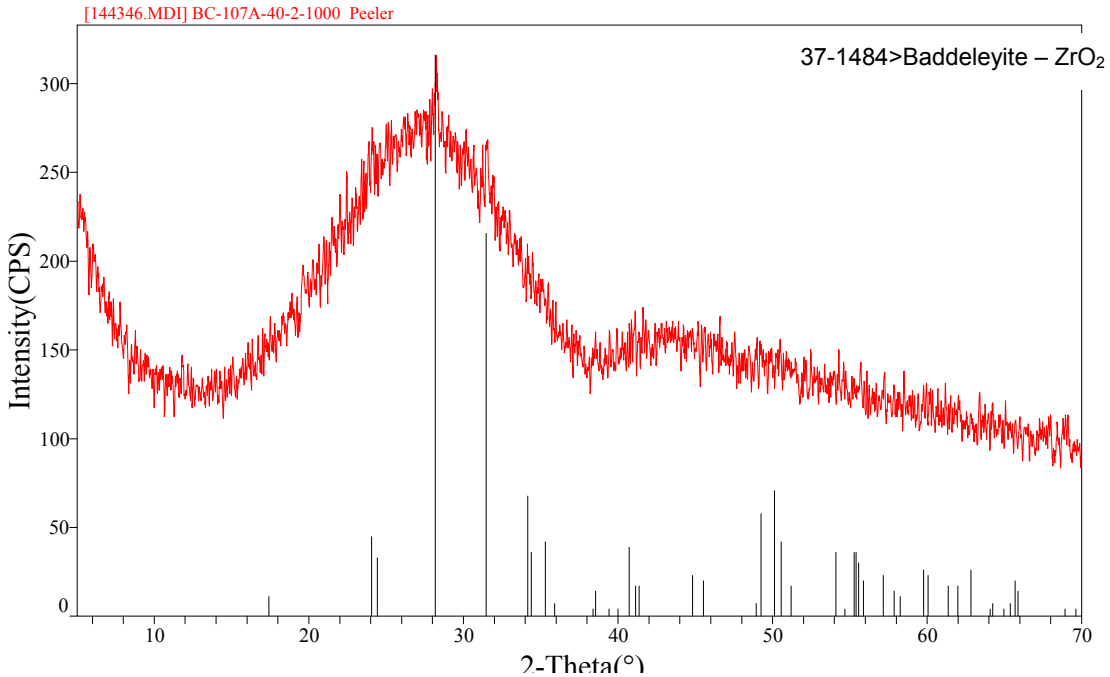

Figure 4-25. XRD Pattern for ML-107A-40-2 After 1 H at 1000°C (remelt)

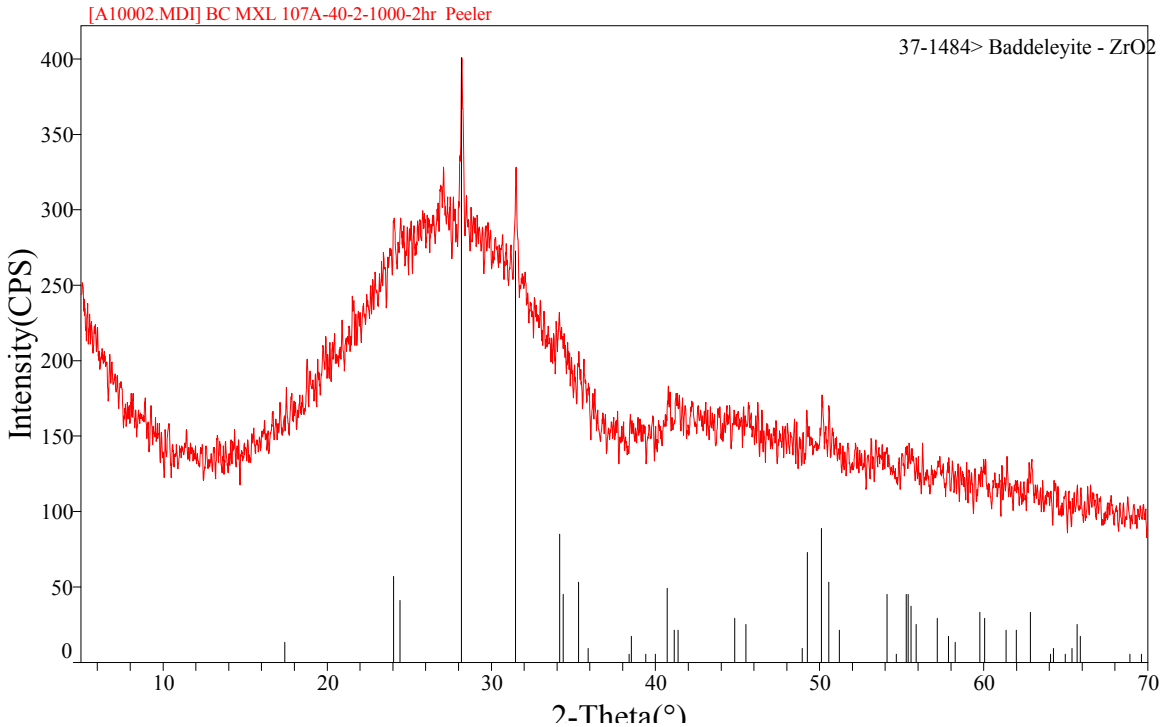

Figure 4-26. XRD Pattern for ML-107A-40-2 After 2 H at 1000°C (remelt)

4.4.9 Melt Behavior

A heterogeneous bubbly layer forms at the batch-melt interface as the granular materials are converted into a melt. This layer is characterized by a large fraction of undissolved refractory particles and gaseous inclusions. The microstructural characteristics and behavior of this layer influence the melting rate of the batch. The rate at which heat is transferred across the interface is related to the rate of batch-to-melt conversion. If no impediment of heat transfer to the batch occurred, reaction kinetics would limit the melting rate. However, the formation of the thermally insulating foam layer (primarily due to the gaseous inclusions) reduces heat transfer from the molten glass to the batch.

To assess the melting behavior of the ML-107A-40 feed material, a series of crucibles were heat treated as a function of temperature. The series of isothermal crucible scale tests is only an approximation of the complex reaction kinetics that will occur in the melter. The objective is to identify 1) temperature regimes in which major volume expansion may occur, 2) the formation of a stable foamy layer, and/or 3) required dissolution times for refractory oxides within the batch.

Nine batches of ML-107A-40 were prepared (targeting 100 g of glass) using oxides, carbonates, and boric acid precursors according to standard procedures. Batches were thoroughly mixed and placed in separate 250 mL Al_2O_3 crucibles (with lids). All nine crucibles were placed in a furnace and ramped at 8°C/min. One crucible was removed at each of the following temperatures: 600°, 700°, 750°, 800°, 850°, 900°, 950°, 1000°, and 1100°C. Crucibles were removed at temperature with no hold and rapidly cooled to room temperature. Table 4.20 summarizes the visual observations of each crucible after cooling to room temperature. Photographs of the melt series are shown in Figure 4-27 through Figure 4-35.

The results of the melt behavior tests indicated no volume expansion or stable foam formation. The batch basically reacted producing intermediate phases, which transitioned into a glassy product at 1100°C. Again, the series ramp heated crucible scale tests is only an approximation of the complex reaction kinetics that will occur in the melter.

Table 4.20. Visual Observations on Melt Behavior Tests

Temperature (°C)	Comments
600	Sintered mass, no batch expansion/reduction, no liquid phase observed
700	Sintered mass, no batch expansion/reduction, no liquid phase observed
750	Initial liquid phase observed, no batch expansion or volume reduction
800	Liquid phase on melt surface, majority of batch still “unreacted,” no volume expansion or reduction observed, large bubbles appear to be trapped in liquid phase
850	Liquid phase on melt surface, majority of batch still “unreacted,” slight volume reduction observed in center of melt, large bubbles appear to be trapped in liquid phase
900	Volume reduction continues, large bubbles trapped within liquid phase, batch appears to be completely converted into an initial liquid
950	No major changes to melt surface, large bubbles trapped at melt surface, liquid near bottom converting to “glass,” volume reduction continues
1000	Small layer of material on surface of melt, most of sample is “glassy,” volume reduction continues
1100	Almost complete glassy state, still have limited amount of intermediate phases on melt surface.

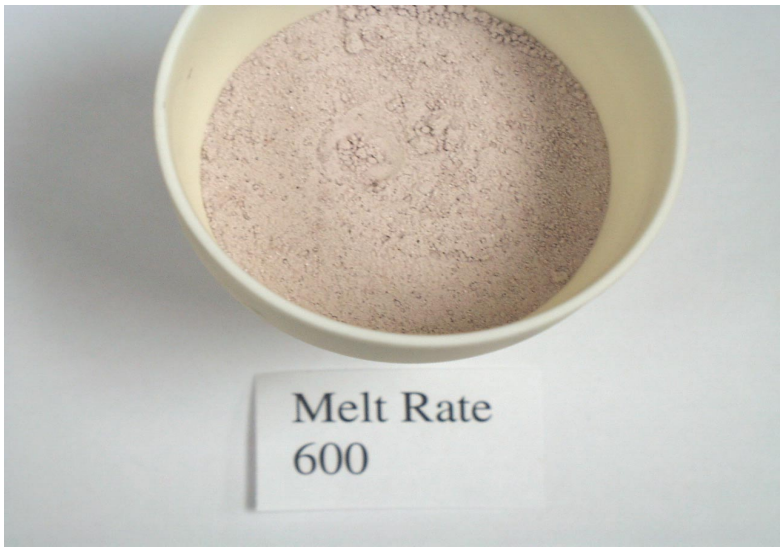

Figure 4-27. ML-107A-40 at 600°C

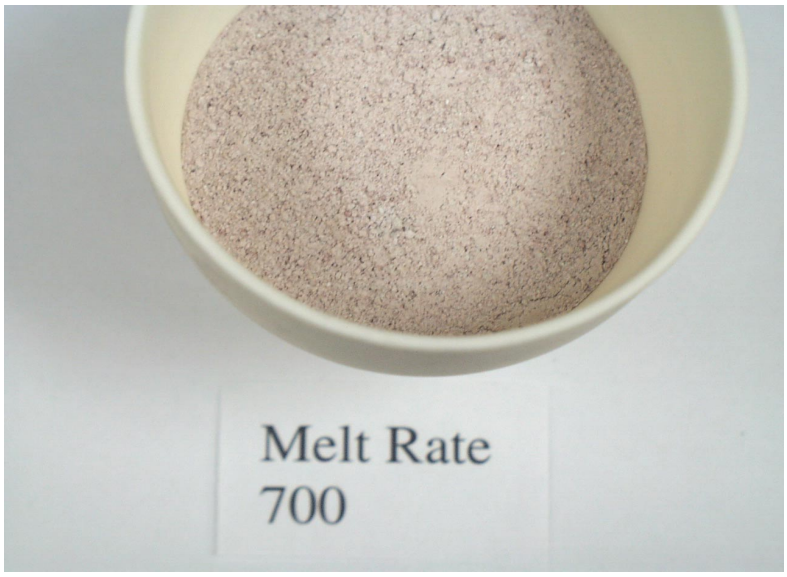

Figure 4-28. ML-107A-40 at 700°C

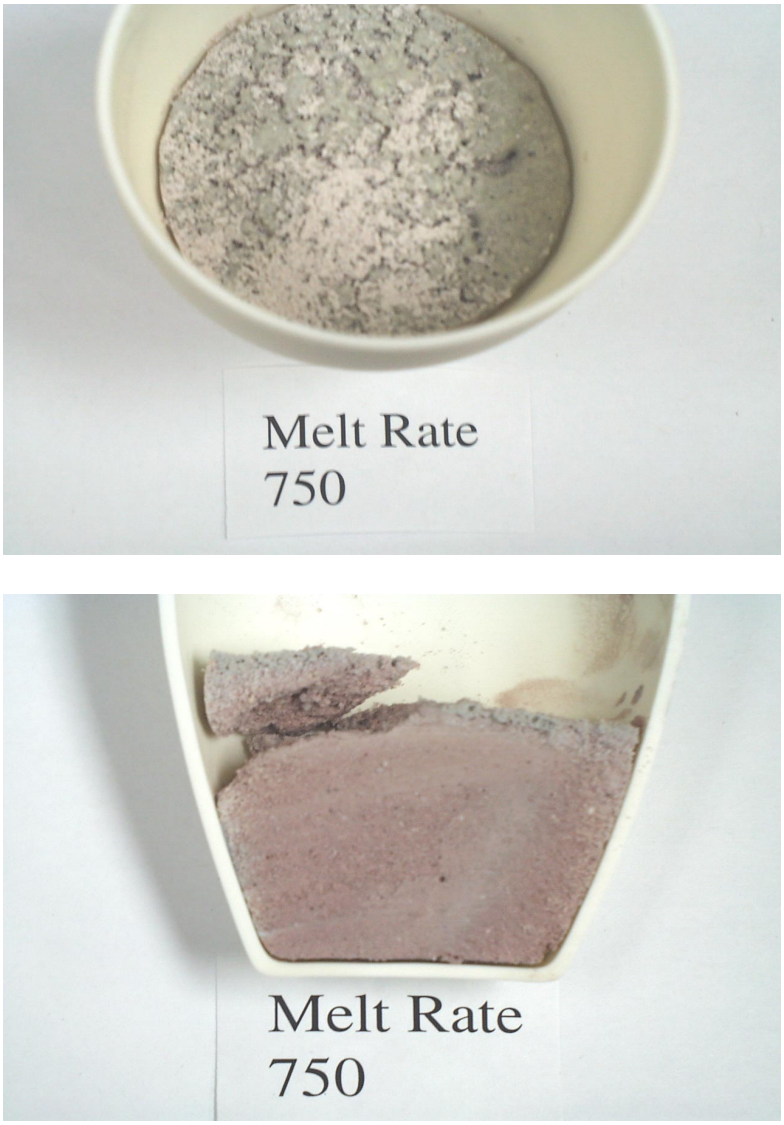

Figure 4-29. ML-107A-40 at 750°C

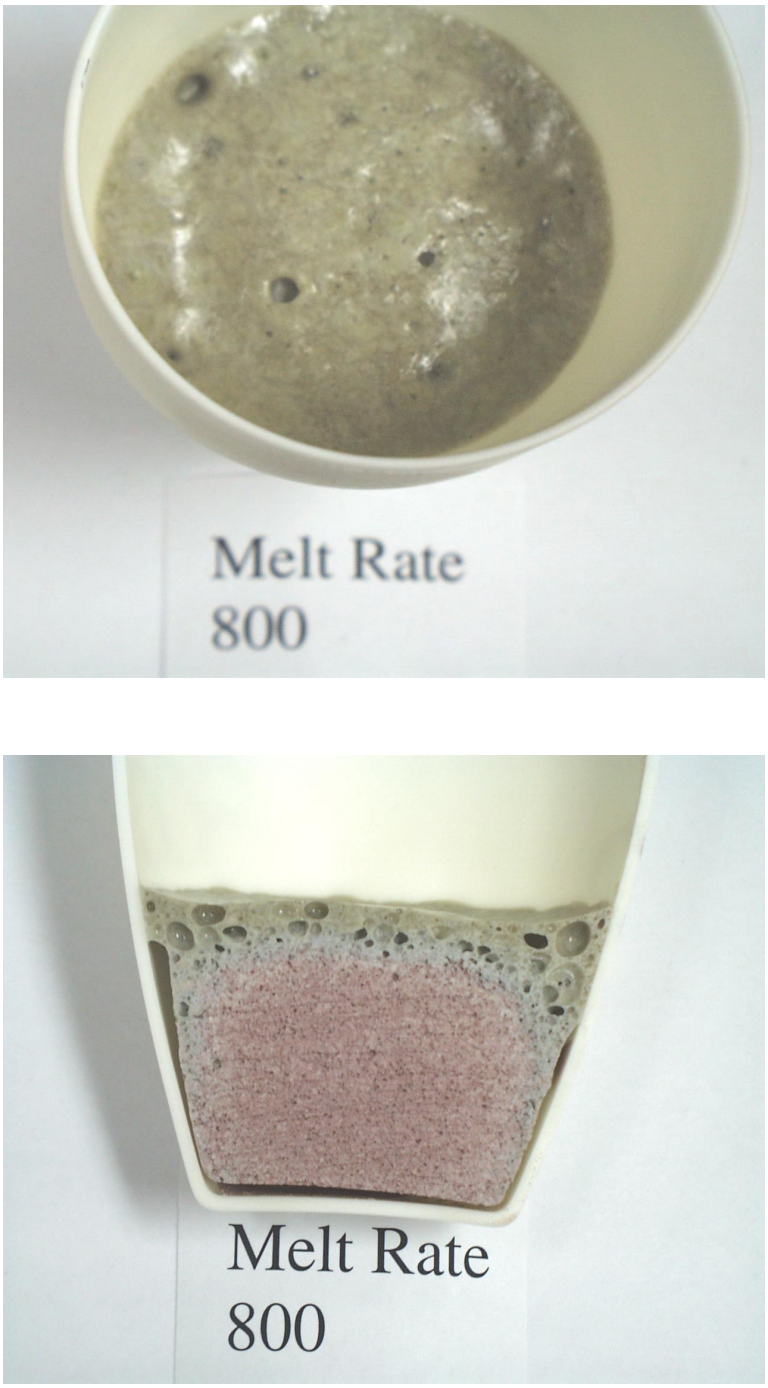

Figure 4-30. ML-107A-40 at 800°C

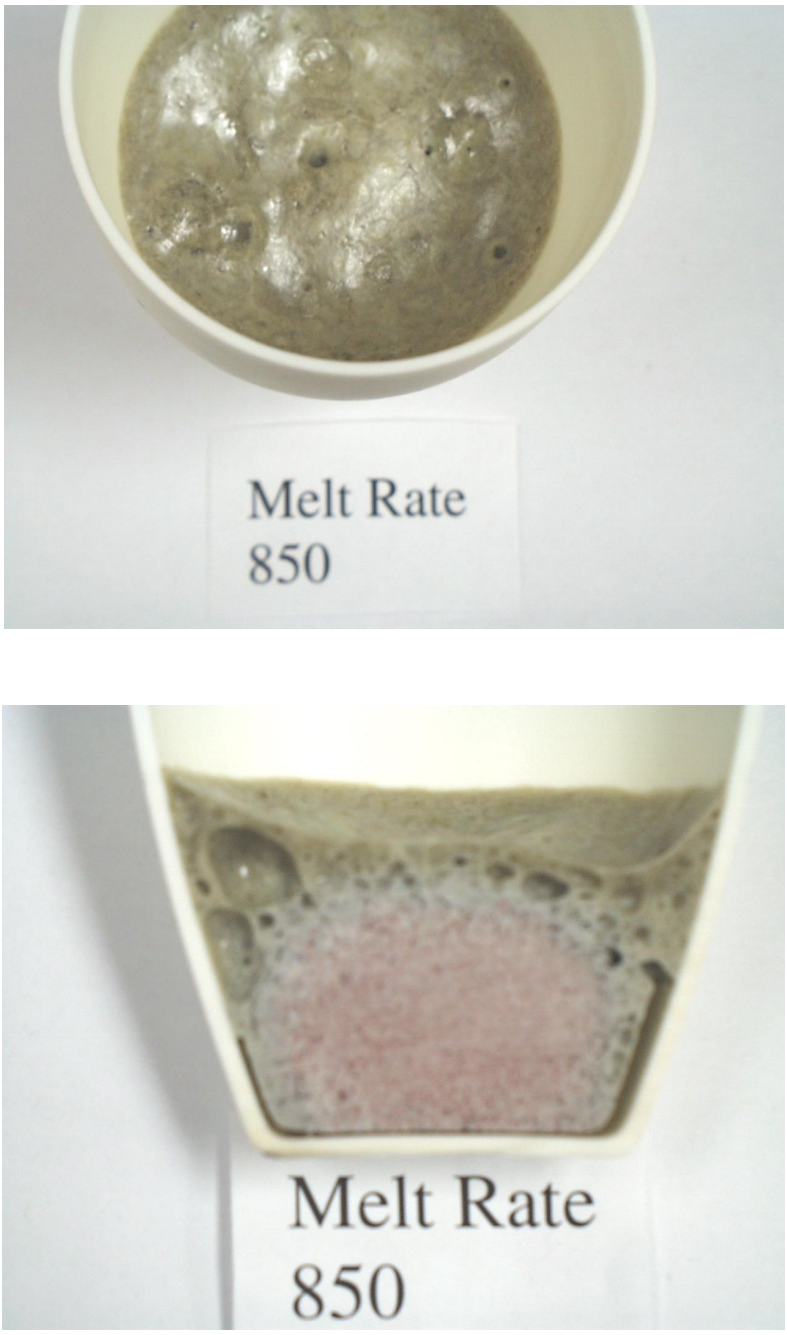

Figure 4-31. ML-107A-40 at 850°C

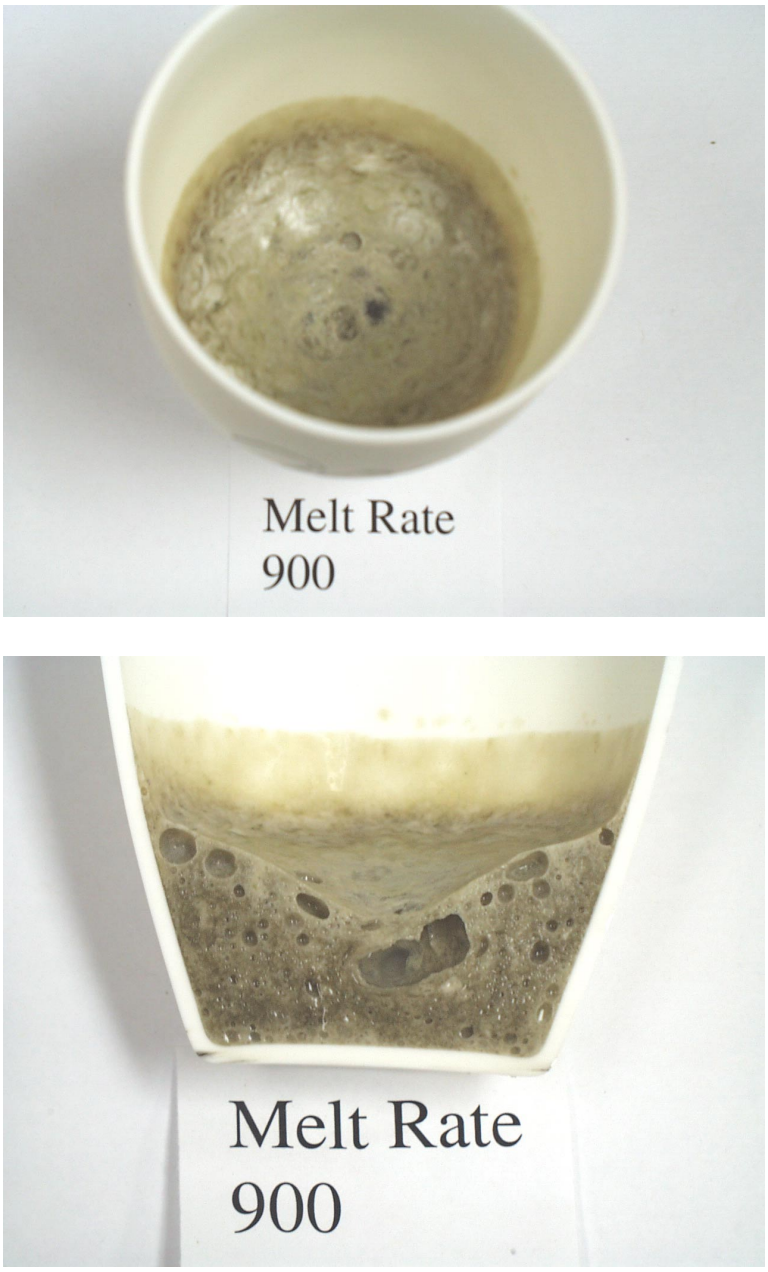

Figure 4-32. ML-107A-40 at 900°C

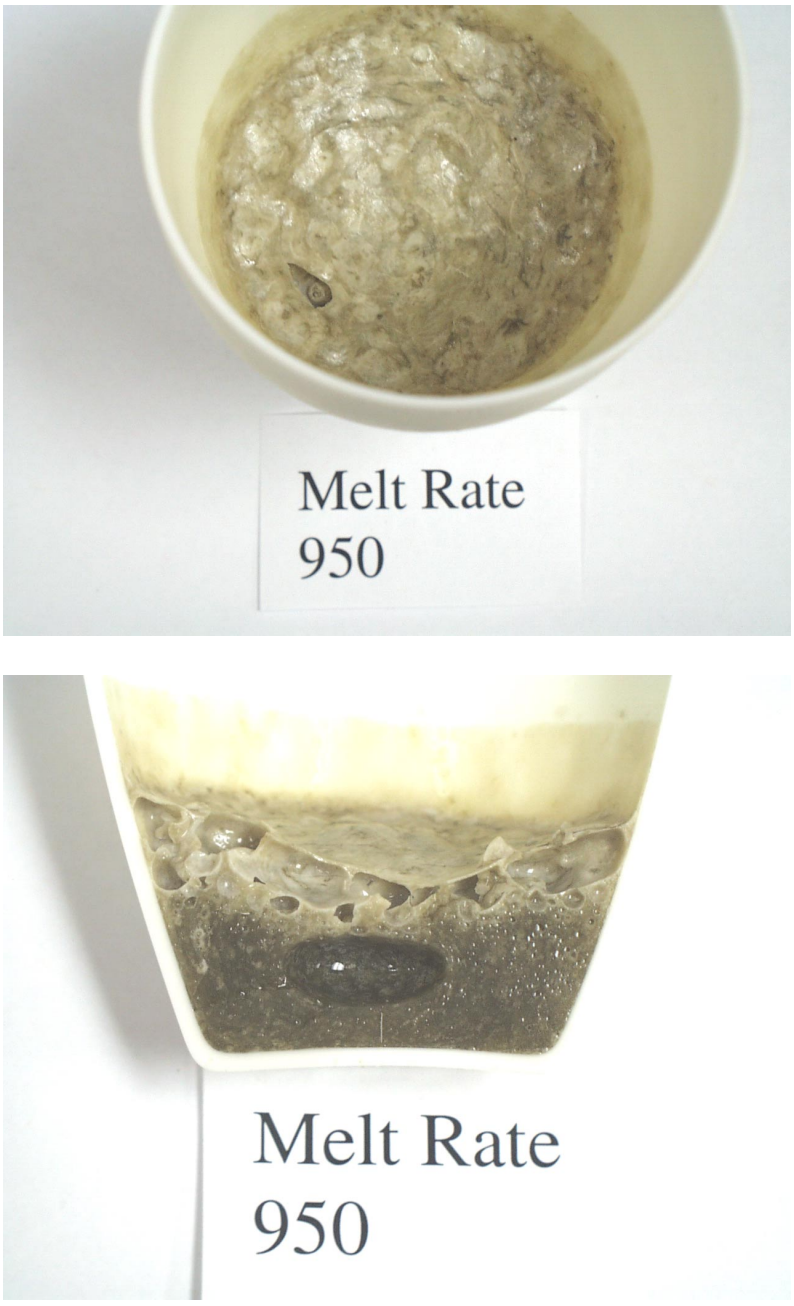

Figure 4-33. ML-107A-40 at 950°C

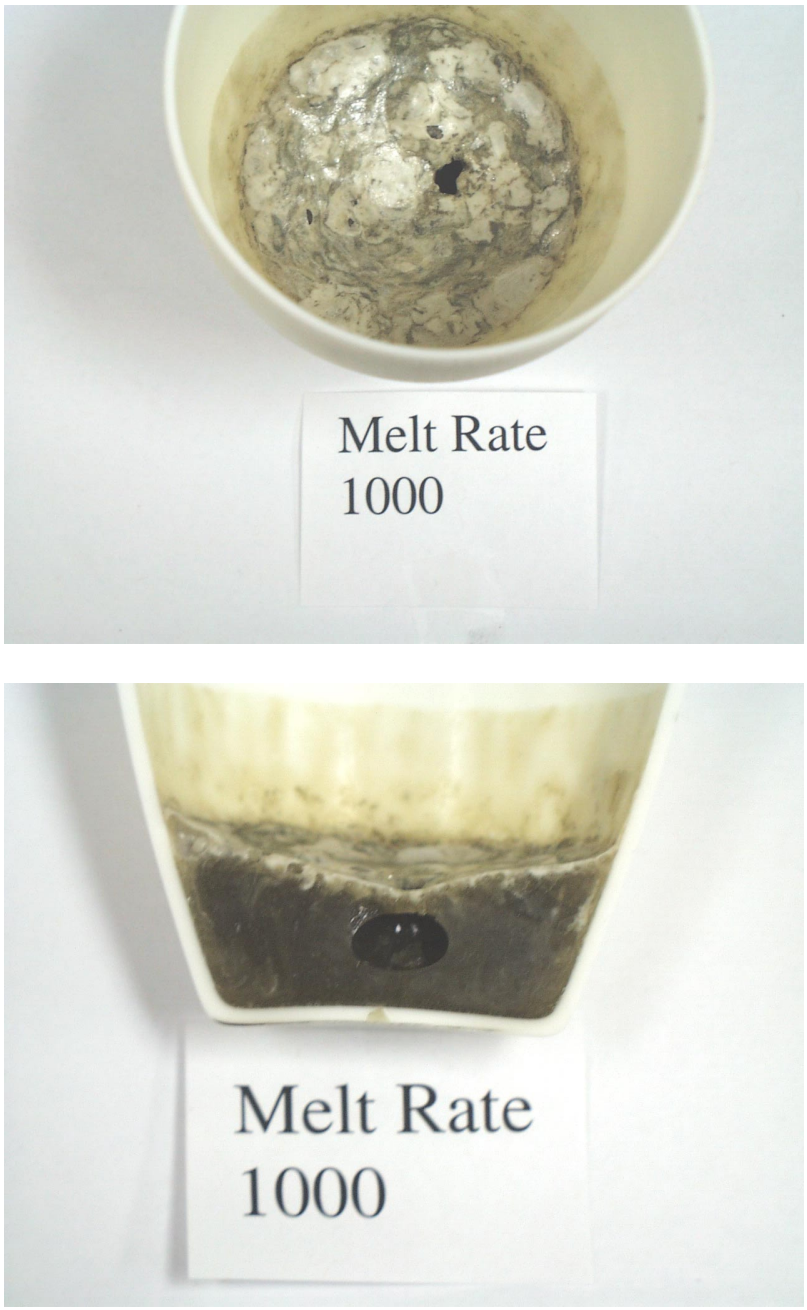

Figure 4-34. ML-107A-40 at 1000°C

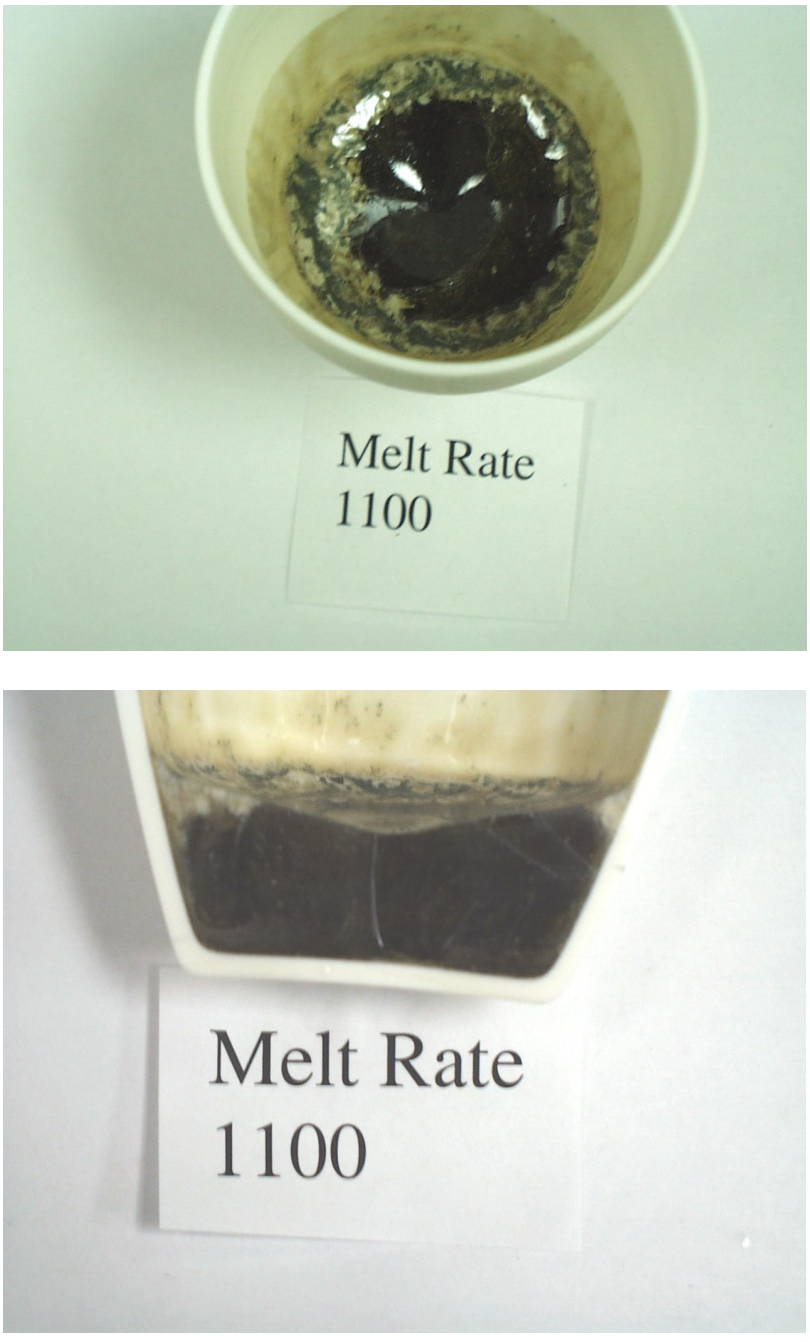

Figure 4-35. ML-107A-40 at 1100°C

4.4.10 Meltability Study

Max WL107-40%WL-MR was batched using oxides and carbonates and boric acid for the frit components along with 40% Blend calcine waste. The chemicals used were portions of the chemicals selected for use in the upcoming melter demonstration. A representative sample of the batch was put into a platinum crucible and placed in the differential thermal analyzer/ thermogravimeteric (DTA/TGA) at room temperature. A gas chromatograph/mass spectrometer (GC/MS) was coupled to the DTA/TGA to identify and quantify the concentration of gases evolved from the sample. Helium was used as a cover gas at 50 mL/min. The sample was ramped at 5°C/min to a temperature of 1150°C. Data were collected on mass loss, temperature, off gas, and temperature difference between the sample and the reference.

Results of the DTA/TGA run in He atmosphere for MaxWL-7-40%WL glass are shown in Figure 4-36. The plot shows the temperature ranges of the gases evolved: CO 100–560°C, CO_2 250–625°C, and NO 450–650°C. Table 4.21 shows the measured weight loss of the sample by DTA/TGA and the measured volumes of CO, CO_2, and NO by the GC/MS. Results of the GC/MS were then converted to masses of each gas and totaled to compare the DTA/TGA results with the GC/MS results. Water was not examined and quantified by the GC/MS because of its inability to stay in a vapor phase.

Table 4.21. Measured Volumes and Masses of each Gas Species Detected by the GC/MS and TGA

mL of CO_2 MS	2.01		mg of CO_2 MS	3.62
mL of NO MS	1.48		mg of NO MS	1.82
mL of CO MS	5.08		mg of CO MS	5.82
total mL offgas MS	8.58		total mg offgas MS	11.26
			total mg offgas TGA	9.67

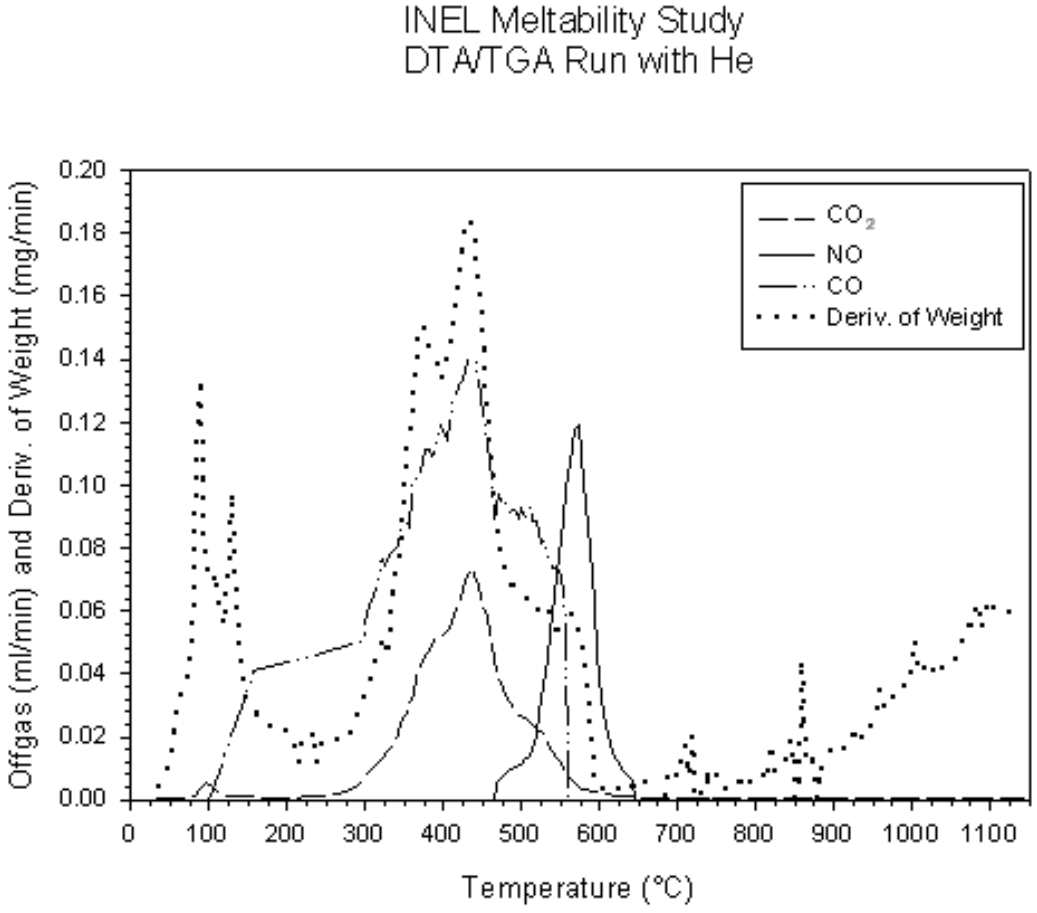

Figure 4-36. Plot of DTA/TGA Run with Off Gas Coupled to the GC/MS

5.0 Recommendations

Frit ML-107 with 40 mass% waste loading of Blend calcine waste is recommended for scaled melter demonstrations of the direct vitrification process of INEEL calcine waste. This glass satisfied all of the formulation constraints except η at T_M=1125 ± 25°C. The viscosity of the glass was below the 2 Pa·s constraint at T_M= 1125 ± 25°C. Although the melt temperature could be lowered based on the measured viscosity curve, the melt temperature should be at or slightly above 1100°C to maintain $T_L = T_M - 100$°C because the T_L=1004°C,. As stated earlier, requiring the T_M to be maintained at 1125 ± 25°C will limit waste loading of future formulation efforts with high F unless an additive can be found that increases F solubility while raising melt temperature. To maintain high fluorine solubility in the glass, the composition region required is a low concentration of SiO_2 and high concentrations of alkalis and/or B_2O_3 and F.

Frit 107 out performed all other frit compositions at 40 wt% loading of Blend calcine waste in terms of crystallization during slow cooling. Quenched glass was free of phase separation and crystallization, and CCC samples crystallized approximately 2 wt% CaF_2. But the potential exists for the glass to highly crystallize at temperatures below 1004°C as seen during the devitrification test at 750°C for 48 h. Also note that fluctuations in waste loading above 40 wt% could result in dramatically higher devitrification of the quenched and/or especially slow cooled glass.

PCT was performed to assess the durability of quenched and CCC samples of Frit 107 glasses containing 40 mass% Blend calcine. The r_i values, normalized to target compositions, are well below those reported for the EA glass as well as the conservative constraint of 1 g/m^2 being used in this study.

No attempt was made to measure the corrosion rates of melter construction materials. This could be an area of concern, especially due to the low η (< 2 Pa·s) of the glass at a T_M of 1100°C.

6.0 References

American Society for Testing and Materials (ASTM). 1998. "Standard Test Method for Determining Chemical Durability of Nuclear Waste Glasses: The Product Consistency Test (PCT)," ASTM-C-1285-97, in *Annual Book of ASTM Standards*, Vol. 12.01, ASTM, WEST Conshohocken, Pennsylvania.

Bailey, W. and P. Hrma. 1995. "Waste Loading Maximization for Vitrified Hanford HLW Blend," *Ceram. Trans*. 61, pp. 549-556, American Ceramic Society, Westerville, Ohio.

Hrma, P. and A. W. Bailey. 1995. "High Level Waste at Hanford: Potential for Waste Loading Maximization," *Proc. 1995 Int. Conf. Nucl. Waste Manag. and Environ. Remediation (ICEM'95),* Vol. 1, pp. 447-451.

Jantzen, C.M., N.E. Bibler, D.C. Beam, C.L. Crawford, and M.A. Pickett. 1993. *Characterization of the Defense Waste Processing Facility (DWPF) Environmental Assessment (EA) Glass Standard Reference material*, WSRC-TR-92-346, Rev. 1, Westinghouse Savannah River Company, Aiken, South Carolina.

Kim, D-S, D. K. Peeler, and P. Hrma. 1995. "Effects of Crystallization on the Chemical Durability of Nuclear Waste Glasses," *Ceram. Trans*. 61, pp. 177-185, American Ceramic Society, Westerville, Ohio.

Li, H., J. D. Vienna, P. Hrma, D. E. Smith, and M. J. Schweiger. 1997. "Nepheline Precipitation in High-Level Waste Glasses - Compositional Effects and Impact on the Waste Form Acceptability," *Scientific Basis for Nuclear Waste Management* (Editors W. J. Gray and I. R. Triay), Vol. 465, pp. 261-268, Material Research Society, Pittsburgh, Pennsylvania.

Marra, S. L. and C. M. Jantzen. 1993. *Characterization of Projected DWPF Glasses Heat Treated to Simulate Canister Centerline Cooling (U),* WSRC-TR-92-142, Rev. 1, Westinghouse Savannah River Company, Aiken, South Carolina.

Mellinger, G.B. and J.L. Daniel. 1984. *Approved Reference and Testing Materials for Use in Nuclear Waste Management Research and Development Programs,* PNL-4955-2, Pacific Northwest National Laboratory, Richland, Washington.

Mohr, C. M., L. O. Nelson, and D. D. Taylor. 2000. *Optimization of Calcine Blending during Retrieval from Binsets,* INEEL/EXT-2000-00896, Idaho National Engineering and Environmental Laboratory, Idaho Falls, Idaho.

Musick, C.A., B.A. Scholes, R.D. Tillotson, D.M. Bennert, J.D. Vienna, J. V. Crum, D.K. Peeler, I.A. Reamer, D. F. Bickford, J. C. Marra, N.L. Waldo. 2000. *Technical Status Report: Vitrification Technology Development Using INEEL Run 78 Pilot Plant Calcine,* INEEL\EXT-2000-00110, Idaho National Engineering and Environmental Laboratory, Idaho Falls, Idaho.

Staiger, M. D. 1999. *Calcine Waste Storage at the Idaho Nuclear Technology and Engineering Center,* INEEL/EXT-98-0045, Idaho National Engineering and Environmental Laboratory, Idaho Falls, Idaho.

U.S. Department of Energy (DOE). 1995. *The INEEL Spent Nuclear and Environmental Restoration and Waste Management Programs Environmental Impact Statement,* DOE\EIS-0202-F, April 1995, U.S. Department of Energy, Washington, D.C.

Distribution

No. of Copies

OFFSITE

2 U.S. DOE / Office of Scientific and Technical Information

1 DOE Idaho Operations Office
750 DOE Place, MSIN: 1145
Idaho Falls, ID 83402
Attn: Kieth Lockie

10 Idaho National Engineering and Environmental Laboratory
P. O. Box 1625
Idaho Falls, ID 83415
Attn: R. R. Kimmitt MS 5218
C. A. Musick (5) MS 5218
A. L. Olson MS 5218
J. Rindfleisch MS 5218
B. A. Scholes MS 5218
J. H. Valentine MS 3211

12 Westinghouse Savannah River Co.
SRTC, Bldg 773-A
Aiken, South Carolina 29808
Attn: D. A. Crowley 773-43A
T. B. Edwards 773-42A
E. W. Holtzscheiter 773-A
C. M. Jantzen 773-A
J. C. Marra 773-43A
S. L. Marra 704-1T
D. K. Peeler (5) 773-43A
I. A. Reamer 773-A

No. of Copies

ONSITE

1 DOE Richland Operations Office
P. O. Box 550, MS: K8-50
Richland, Washington 99352
Attn: T. P. Pietrok K8-50

2 PHMC, Hanford
Attn: J. O. Honeyman R2-58
S. L. Lambert R3-75

27 Pacific Northwest National Laboratory
T. M. Brouns K9-69
W. F. Bonner K9-14
J. L. Buelt K9-09
J. V. Crum K6-24
P. Hrma K6-24
D-S. Kim K6-24
J. M. Perez H6-61
L. M. Peurrung K6-24
G. F. Piepel K5-12
J. D. Vienna(5) K6-24
B. J. Williams (TFA) (8) K9-69
Technical Report Files (5) P8-55